Engineering 41 (2024) 110–129

Contents lists available at ScienceDirect

Engineering

journal homepage: www.elsevier.com/locate/eng

Research
Civil Engineering—Feature Article

Recent Construction Technology Innovations and Practices for Large-Span Arch Bridges in China

Jielian Zheng *

School of Civil Engineering and Architecture, Guangxi University, Nanning 530004, China

ARTICLE INFO

Article history:
Received 31 October 2023
Revised 13 April 2024
Accepted 19 May 2024
Available online 21 June 2024

Keywords:
Concrete-filled steel tubular arch bridges
Steel-reinforced concrete arch bridges
Cable-stayed fastening-hanging cantilevered assembly
Non-rocky thrust abutment foundation
Stiff skeleton
Encasing concrete pouring
Longitudinal reinforcement optimization

ABSTRACT

Arch bridges provide significant technical and economic benefits under suitable conditions. In particular, concrete-filled steel tubular (CFST) arch bridges and steel-reinforced concrete (SRC) arch bridges are two types of arch bridges that have gained great economic competitiveness and span growth potential due to advancements in construction technology, engineering materials, and construction equipment over the past 30 years. Under the leadership of the author, two record-breaking arch bridges—that is, the Pingnan Third Bridge (a CFST arch bridge), with a span of 560 m, and the Tian'e Longtan Bridge (an SRC arch bridge), with a span of 600 m—have been built in the past five years, embodying great technological breakthroughs in the construction of these two types of arch bridges. This paper takes these two arch bridges as examples to systematically summarize the latest technological innovations and practices in the construction of CFST arch bridges and SRC arch bridges in China. The technological innovations of CFST arch bridges include cable-stayed fastening-hanging cantilevered assembly methods, new in-tube concrete materials, in-tube concrete pouring techniques, a novel thrust abutment foundation for non-rocky terrain, and measures to reduce the quantity of temporary facilities. The technological innovations of SRC arch bridges involve arch skeleton stiffness selection, the development of encasing concrete materials, encasing concrete pouring, arch rib stress mitigation, and longitudinal reinforcement optimization. To conclude, future research focuses and development directions for these two types of arch bridges are proposed.

© 2024 THE AUTHOR. Published by Elsevier LTD on behalf of Chinese Academy of Engineering and Higher Education Press Limited Company. This is an open access article under the CC BY-NC-ND license (http://creativecommons.org/licenses/by-nc-nd/4.0/).

1. Introduction

The arch bridge, as one of the four main bridge types alongside the beam bridge, cable-stayed bridge, and suspension bridge, is distinguished not only by its elegant aesthetic form but also by its superior structural performance. Provided that the constant loads (i.e., the self-weight of the structural components) are appropriately arranged and the arch axis is well designed, the arch ring will be under axial compression when subjected to constant loads only and will be under small eccentric compression when subjected to a standard combination of constant loads and live loads. As a result, arch bridges are well known for their resilience against fatigue-related problems and have outstanding durability and impressive stiffness. For example, the Anji Bridge in Hebei Province, China, which was constructed over 1400 years ago, remains steadfast today. The Lugou Bridge, built in China 800 years ago, has successfully endured the test of a 400 t flatbed truck without any noticeable damage. These historical instances unequivocally show the long durability and remarkable load-bearing capacity of arch bridges. Nonetheless, the arch bridge has shortcomings, too. Its construction cost and risks are high due to the arch ring's curved shape, substantial mass, and heavy reliance on a large number of temporary construction facilities. Moreover, with extension of the arch span length, these shortcomings become even more pronounced, hindering the construction of arch bridges with longer spans.

The history of arch bridge construction reveals that this bridge's span length increases and construction cost reduction rely heavily on construction technology innovations. To this end, Chinese engineers have carried out extensive research and practice to tackle challenges related to arch bridge construction, such as arch ring erection and construction risk mitigation, in addition to methods to reduce the cost of temporary construction facilities. These efforts have yielded significant economic benefits and a succession of innovative technologies for arch bridge construction.

* Corresponding author.
E-mail address: tubing2018@gxu.edu.cn (J. Zheng).

https://doi.org/10.1016/j.eng.2024.05.019
2095-8099/© 2024 THE AUTHOR. Published by Elsevier LTD on behalf of Chinese Academy of Engineering and Higher Education Press Limited Company.
This is an open access article under the CC BY-NC-ND license (http://creativecommons.org/licenses/by-nc-nd/4.0/).

Over the past three decades, China has undertaken ambitious endeavors in highway and high-speed railway construction; hence, there has been a substantial surge in the demand for arch bridges—especially large-span arch bridges. Thanks to significant advancements in the techniques, materials, and equipment used in arch bridge construction, China currently holds all the world records for the span length of all types of arch bridges, including steel arch bridges, concrete-filled steel tubular (CFST) arch bridges, concrete arch bridges, highway arch bridges, and railway arch bridges. As of 2022, China boasts a total of 167 186 highway arch bridges. However, these constitute only 16.2% of the entire highway bridge inventory, falling far short of the proportion this exceptional bridge type deserves.

Over the past 30 years, the author's team has dedicated its efforts to research on CFST arch bridges and steel-reinforced concrete (SRC) arch bridges. It has been found that these two types of arch bridges not only inherit the general features of arch bridges but also possess several other notable comparative advantages, including high efficiency in construction, low sensitivity to temperature fluctuations, low temperature stress, easy extension of span length, and high economic benefits. Noteworthy breakthroughs have been made in the realms of both construction technology and practical implementation for these two types of arch bridges. The span length of the CFST arch bridges and SRC arch bridges constructed in China far surpasses those built outside China, and independent intellectual property rights have been gained. Detailed information on the innovations in CFST and SRC arch bridges made by Chinese engineers over the past 30 years can be found in Ref. [1].

In the past five years, the author presided over the construction of two world-record-breaking arch bridges: the Pingnan Third Bridge, with a span of 560 m, and the Tian'e Longtan Bridge, with a span of 600 m. Construction of the Pingnan Third Bridge started on August 2018, and the bridge was opened to traffic by the end of 2020, demonstrating a new pinnacle in the construction technology of super-large-span CFST arch bridges. Dr. Wenzhong Deng, an academician of the National Academy of Engineering in the United States and a foreign academician of the Chinese Academy of Engineering, commented, "The successful construction of the Pingnan Third Bridge comprehensively validates China's nearly three decades of technological expertise in the domain of CFST arch bridges. It represents the zenith of modern CFST arch bridge construction." The Tian'e Longtan Bridge significantly increased the world span record of SRC arch bridges from 445 to 600 m. Construction on this bridge began on 10 June 2020, and the bridge was opened to traffic on 1 February 2024. During the construction of these two grand arch bridges, numerous new technical challenges emerged, and corresponding solutions were proposed after in-depth investigations. The subsequent two sections will delve into the technological innovations and practices associated with CFST arch bridges and SRC arch bridges during these five years.

2. CFST arch bridges

A CFST arch bridge is an arch bridge with a CFST arch or a truss arch with CFST chords. In a CFST arch, the in-tube concrete serves to maintain the local stability of the steel tubes, while the steel tubes, in turn, confine the concrete and thereby increase the concrete's strength and ductility. Such a synergy creates an excellent steel–concrete composite structure. Furthermore, the amount of steel used for a large-span CFST arch rib is generally only half of that used for a steel truss arch bridge. The other half of the steel that would be used on a steel truss arch bridge is replaced by concrete within steel tubes in a CFST arch bridge to bear the compressive force. These steel tubes function as both a skeleton and a formwork. Consequently, the CFST arch bridge boasts greater cost-effectiveness and a lighter installation weight in comparison with traditional steel arch bridges. Moreover, since the CFST arch is a self-supporting structure, the steel tube arch rib is erected before the in-tube concrete is poured. This construction approach places the steel tubes under loading first and thus gives full play to the high-strength attributes of the steel tubes within the composite structure, making the CFST arch a highly desirable load-bearing structure. Therefore, CFST arch bridges provide significant technical and economic benefits under certain conditions.

Based on a statistic analysis of the five super-large-span CFST arch bridges constructed recently by the Guangxi Road and Bridge Engineering Group Corporation (China), there is an average cost reduction of 25% of CFST arch bridges compared with cable-stayed bridges with the same span length. Consequently, despite fierce competition in the bridge construction market in China, nearly 500 CFST arch bridges have been built over the past three decades, among which 51 bridges have a span over 300 m and 19 bridges have a span over 400 m, as detailed in Table 1. Remarkably, nearly 100 CFST bridges were constructed within the past four years.

The latest research progress in and construction practices for large-span CFST arch bridges will be elucidated in the following section, taking the Pingnan Third Bridge as an example. These facets encompass arch rib fabrication and erection, new in-tube concrete development, in-tube concrete pouring, abutment foundation treatment in non-rocky terrain, and optimization of large-scale temporary construction facilities.

2.1. Overview of the Pingnan Third Bridge

The Pingnan Third Bridge is a super-long arch bridge in Guangxi Zhuang Autonomous Region, China; it spans the Xunjiang River on the Lipu–Yulin Expressway interchange and has a total length of 1105 m. Its main span is a half-through CFST arch bridge. The 560 m span length of the bridge set the world record among all kinds of arch bridges when it was completed. The bridge has a width of 35 m and a rise-span ratio of 1/4. The steel tube arch truss weighs a total of 8440 tonnes and is divided into 44 segments, with the heaviest segment weighing 214 tonnes and measuring 37.1 m in length. To mitigate cumulative error during segment fabrication and to ensure precise connection, coupled horizontal preassembly was utilized. The segments were installed by means of the cable-stayed fastening-hanging cantilevered assembly technique. The chord tubes of the arch truss, each with a diameter of 1400 mm, were filled with concrete via a four-level vacuum-assisted pressure pumping system. With this innovative technique, the in-tube concrete pouring of a total volume of 958 m^3 for a single tube can be completed continuously within 12 h. Fig. 1 shows the results of the ultrasonic test of the No. 1 arch truss chord of the Pingnan Third Bridge at the age of 7, 14, 28, and 715 days after pouring. The results show that the ultrasonic wave velocities at all the time points fall within the range of 4600–5100 m per second, which are larger than the threshold of 4500 m per second for a compact CFST, summarized based on full-scale segment model experiments. Moreover, there are negligible differences between the ultrasonic wave velocities in the vertical and horizontal directions. These results not only confirm the absence of delamination and voids between the concrete and the steel tube but also indicate the presence of concrete pressure being exerted against the tube wall.

The traffic beams feature a composite structure of steel girder grids with a steel–concrete overlay. The steel girder grids were divided into 37 segments to facilitate installation. Both the steel arch truss segments and the steel girder grid segments were prefabricated at a shop in Guangdong Province, China, and transported to the bridge site via shipping. The construction of

Table 1
List of CFST arch bridges with spans greater than 400 m.

No.	Bridge	Main span (m)	Bridge type	Year of completion
1	Pingnan Third Bridge	560	Half through	2020
2	Bosideng Bridge	518	Half through	2013
3	Hejiang Yangtze River Highway Bridge	507	Flying swallow type	2021
4	Dejiang–Yuqing Highway Wujiang River Bridge	504	Deck arch	2023
5	Wushan Yangtze River Bridge	492	Half through	2005
6	Daxiaojing Bridge	450	Deck arch	2019
7	Lhasa–Nyingchi Railway Zangmu Yarlung Tsangpo River Bridge	430	Half through	2021
8	Zhijing River Bridge	430	Deck arch	2009
9	Renhuai–Zunyi Highway Dafaqu Bridge	410	Deck arch	2022
10	Qianwei Minjiang River Bridge	400	Half through	2021
11	Liancheng Bridge	400	Half through	2007
12	Xiniu Heihui River Bridge	518	Deck arch	Under construction
13	Huangtong–Baise Railway Hongshui River Bridge	512	Deck arch	Under construction
14	Leye–Wangmo Highway Yazhe Hongshui River Bridge	508	Half through	Under construction
15	Sichuan–Xizang Railway Jinsha River Bridge	500	Deck arch	Under construction
16	Ninglang–Shangri La Highway Luoji River Bridge	420	Half through	Under construction
17	Zhenba–Guang'an Highway Baima Qujiang River Bridge	418	Half through	Under construction
18	Pingshan Second Minjiang River Bridge	410	Half through	Under construction
19	New Chongqing–Hunan Highway Shuangpu Bridge	405	Deck arch	Under construction

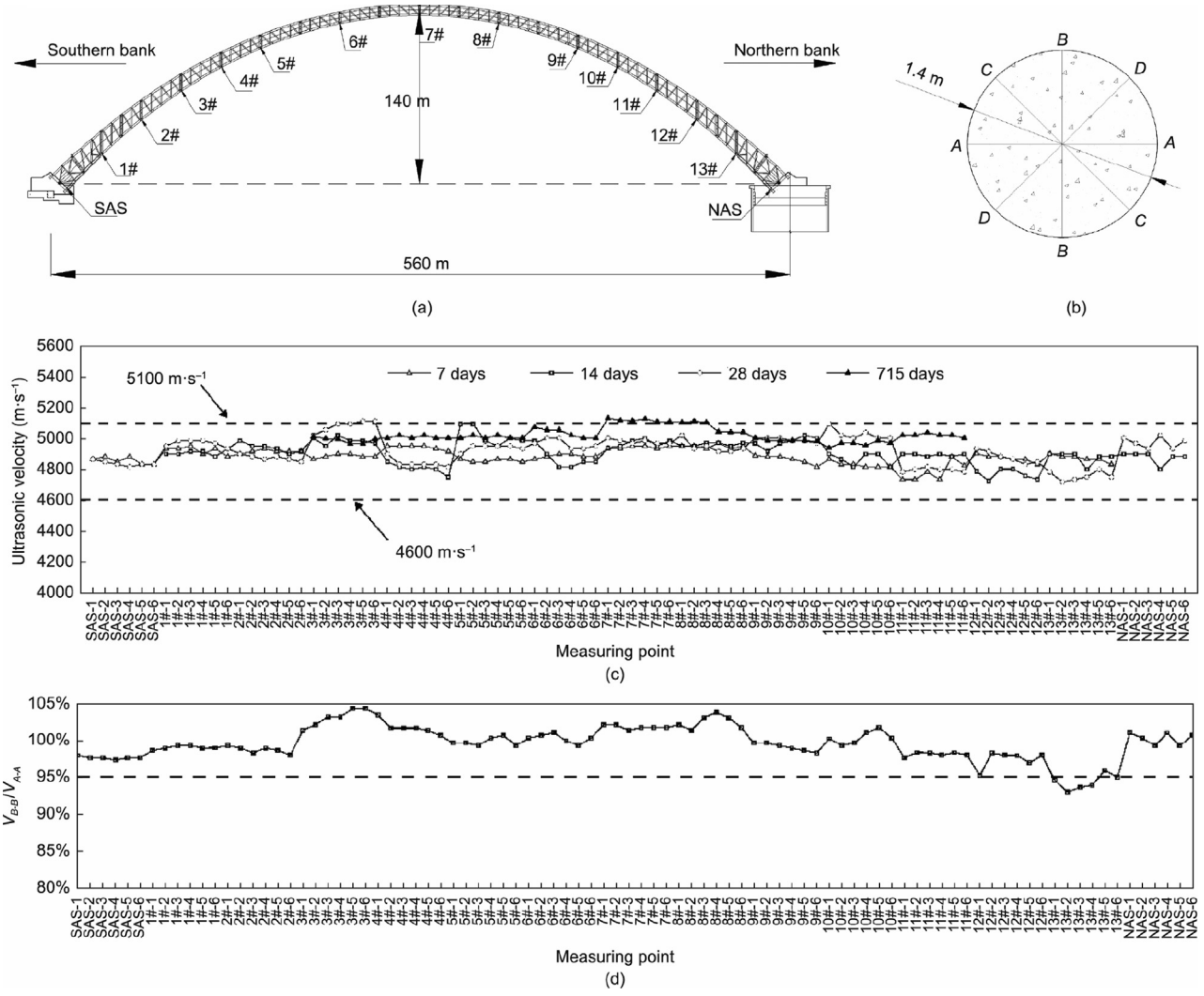

Fig. 1. Ultrasonic testing results of the main arch of the Pingnan Third Bridge. (a) Test section settings; (b) measuring point layout within each arch truss chord; (c) measured ultrasonic wave velocities at several concrete ages of the No. 1 arch truss chord in the *B*–*B* direction; (d) ratio between the measured ultrasonic wave velocities of the No. 1 chord in the *B*–*B* direction (V_{B-B}) and those in the *A*–*A* direction (V_{A-A}) at 28 days. SAS: southern arch springing; NAS: northern arch springing.

the superstructure of the Pingnan Third Bridge lasted for 402 days, as shown in Table 2, which was far less than the time required for a cable-stayed bridge or a suspension bridge with the same span length. The stress and deformation of the main arch upon completion are shown in Fig. 2. The whole construction period of the bridge was 28 months, and the total cost was 545.01 million CNY, which was within the initial budget of the contract. The whole construction process was free from safety incidents, and the bridge was evaluated as achieving excellent quality at the final acceptance. The completed Pingnan Third Bridge is shown in Fig. 3.

It can be seen that the Chinese engineers' decades of in-depth research on CFST arch bridges have been translated into the successful construction of bridges and the establishment of relevant national and industrial specifications. The CFST arch bridge has been developed into a highly competitive type of arch bridge, with the Pingnan Third Bridge as an excellent illustration. Given their

Table 2
Overview of the construction time of the Pingnan Third Bridge.

Construction phase	Start time (month/day/year)	Complete time (month/day/year)	Duration (d)
Overall construction	8/7/2018	12/27/2020	873
Arch rib erection	10/12/2019	1/10/2020	90
In-tube concrete filling	4/17/2020	5/12/2020	25
Traffic beam installation	7/4/2020	9/1/2020	59
Removal of the arch erection system	9/5/2020	11/1/2020	57
Bridge deck paving construction	9/2/2020	11/19/2020	78
Load test	12/26/2020	12/27/2020	2

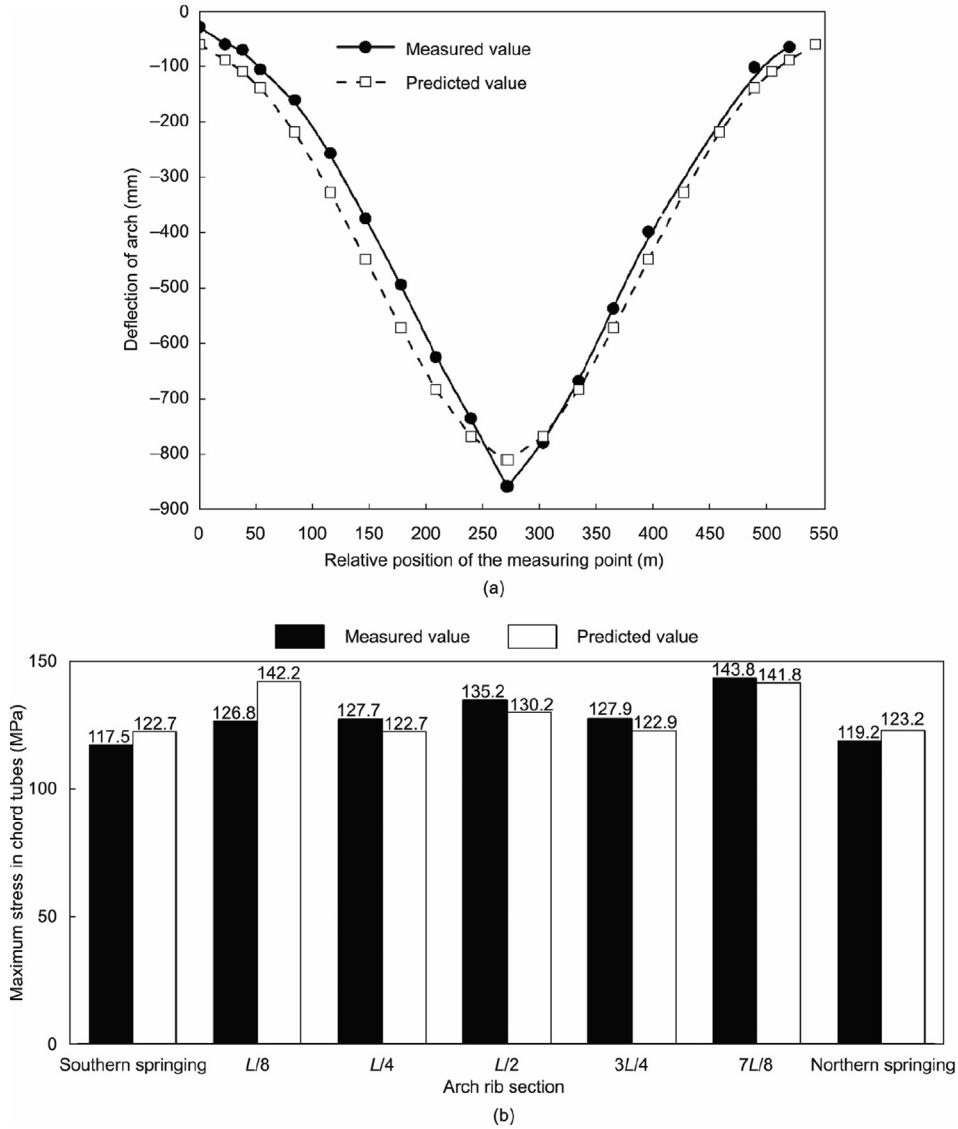

Fig. 2. Critical deformation and stress properties of the main arch of the Pingnan Third Bridge at the bridge completion stage. (a) Deflections of main arch; (b) maximum stresses in the steel tubes of the chords. *L*: span length of the bridge.

Fig. 3. Photograph of the Pingnan Third Bridge.

capacity for the shop prefabrication of arch segments and accessibility to water transportation, CFST arch bridges are the preferable choice among all arch bridges. In 2014, research on the feasibility of building a 700 m-span CFST arch bridge was conducted by the author and colleagues [2]. In this paper, the authors pointed out the possibility of building a CFST bridge with an even larger span. Nonetheless, it should be noted that, as of 2022, the total number of existing bridges with a span length greater than 700 m was only 116, indicating that the market demand for 700 m-span CFST arch bridges is limited.

2.2. Cable-stayed fastening-hanging cantilevered assembly of a steel tube arch truss

In 1968, the author proposed a method for erecting the hyperbolic arches of bridges [3]; this method is called cable (steel rope)-stayed fastening-hanging cantilevered assembly with pre-closure cable loosening (Fig. 4). This innovative method initiated the use of bracket-free construction for arch bridges. The bridge structure realizes its system transformation from cantilever beams to the fixed arch during the relaxation of the buckle cables and lifting cables. The axial compression in the arch is formed concurrently with the gradual removal of cable support, which is similar to the method of erecting an arch on brackets. Consequently, the internal forces of the arch rib are akin to those when an arch is constructed on brackets. This bracket-free approach stands out due to its simple, swift, and cost-effective characteristics. Construction practice has shown that the unit cost of a 100 m-span CFST arch bridge constructed with this method is comparable to that of a 30 m-span simply supported concrete beam bridge.

In 1994, another arch erection method called cable (steel strand)-stayed fastening-hanging cantilevered assembly with post-closure cable loosening was introduced (Fig. 5) [3]. In this method, the arch is fastened and consolidated segment by segment, with precise arch closure in a stress-free state. Following the release and removal of the buckle cables, the erection of the whole arch rib is completed. The bridge structure realizes its system transformation from cantilever beams to the arch in a static state. Therefore, the internal forces in the arch rib equate to the sum of the forces in the cantilever beam and the forces generated by the relaxation of the buckle cables on the arch. Theoretically, this method can be used to assemble any arch bridge, regardless of the span length and the number of segments to be assembled together.

In recent years, the Sichuan Highway Planning, Survey, Design, and Research Institute, Ltd. (China), invented a new type of steel tube arch truss segment with double vertical braces during the design of the Wushan Yangtze River Bridge, as shown in Fig. 6. This new type of segment is only one-third the weight of a conventional arch segment. It also reduces the total amount of high-altitude welding by one-third, mitigating substantial construction risks. Moreover, with the previous segment being preliminarily connected just by flanges, the following segment can be erected immediately. Thus, erection can be done in a rapid and continuous manner. Each segment can be erected within one day, saving construction time.

Based on incomplete statistics, more than 70% of the completed CFST arch bridges have employed cable-stayed fastening-hanging cantilevered assembly methods [4]. Among the 51 CFST arch bridges with a span over 300 m, 50 were constructed via cable-stayed fastening-hanging cantilevered assembly with post-closure cable loosening. It should be pointed out that rotation construction is also a well-established approach for arch rib

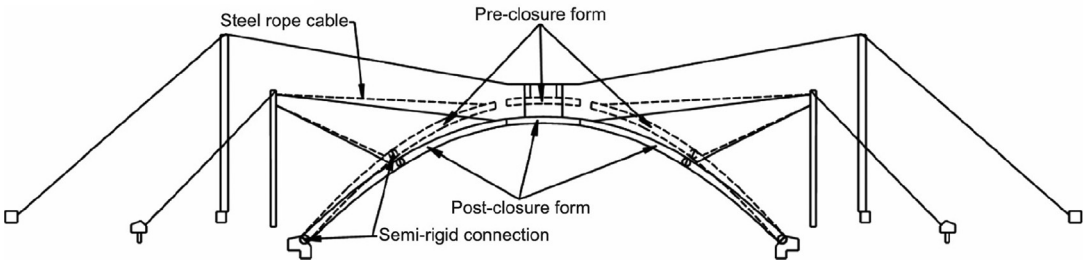

Fig. 4. Diagrammatic sketch of the cable (steel rope)-stayed fastening-hanging cantilevered assembly method with pre-closure cable loosening.

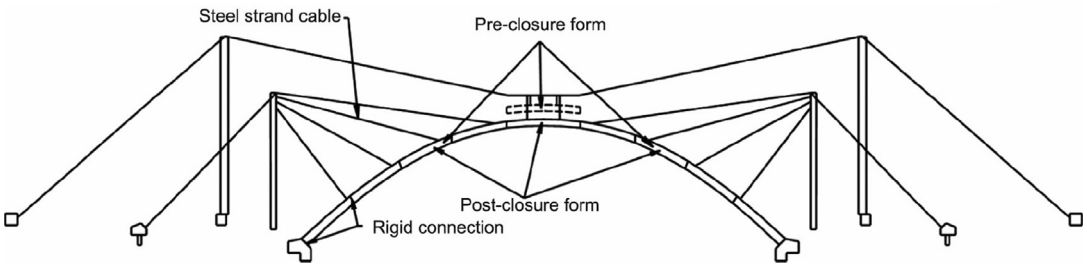

Fig. 5. Diagrammatic sketch of the cable (steel strand)-stayed fastening-hanging cantilevered assembly method with post-closure cable loosening.

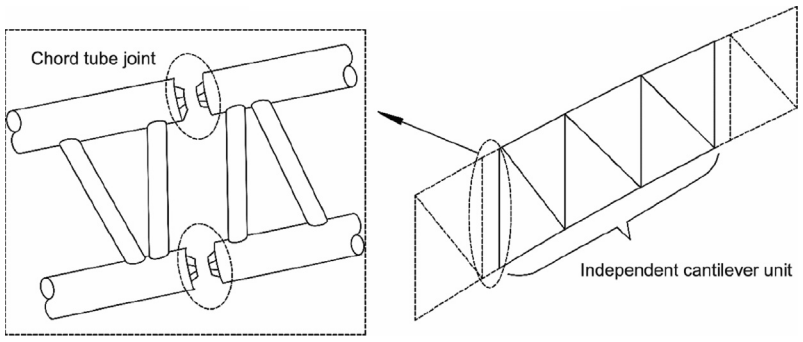

Fig. 6. Novel structure for suspended splicing segments of a steel arch truss with double vertical braces.

erection. Thus, the choice of an appropriate erection method depends on the specific conditions and requirements.

Concerning the fabrication of steel tube arch truss segments, shop fabrication is the preferred choice. In situations where the transportation of segments becomes impractical, shop fabrication of segment components is recommended. Empirical evidence has shown that, whether fabricated at the shop or on the construction site, arch segments should be pre-coupled before erection in order to eliminate cumulative error during fabrication and ensure the precision of the junctions between adjacent segments.

2.3. Development of in-tube concrete materials and pouring techniques

The continuous pouring of concrete within the steel tubes is a fundamental requirement to ensure the structural integrity and construction efficiency of CFST arch ribs. In 1994, during the construction of the Yongning Yong River Bridge, the Guangxi Road and Bridge Engineering Group Corporation proposed a method for the continuous pouring of the in-tube concrete of CFST arch bridges. This innovative approach involves pumping concrete from the two arch springings toward the arch crown, and then filling the steel tube with concrete by its gravity. Later, in response to the challenges posed by a large concrete volume and the lifting height of in-tube concrete during large-span arch bridge construction, a multi-level lifting and pouring method was developed. This method effectively minimizes concrete blockage in the tube. The specific length of each level is determined based on due consideration to the pouring rate and the loss rate of concrete's working performance. To address the problems of voids and inadequate compaction due to air entrapment and buoyancy during the continuous pumping of concrete into the steel tubes, the author introduced the vacuum-assisted pressure pumping method. This method involves the installation of vacuum equipment at the top of the arch ribs to extract air from within the tube in order to create a quasi-vacuum condition with the internal air pressure reduced to 0.01–0.03 MPa. Thus, the method significantly enhances the compaction and pouring rate of in-tube concrete [5,6].

The pouring of in-tube concrete typically involves concrete with a low water–cement ratio and high viscosity, and a long pumping distance. Thus, the degree of compaction strongly depends on the attributes of the concrete, such as the flow capacity, uniformity, and temporal stability. Accordingly, Liu et al. [7] developed a type of concrete admixture that can control the working performance of in-tube concrete by means of the application of carboxyl and alkali-responsive ester-based materials known for their robust thixotropic properties. This new type of admixture-added concrete harmonizes the characteristics of high consistency, low viscosity, high flow capacity, and high resistance against segregation, thereby reducing the concrete's susceptibility to fluctuations in factors such as raw materials, temperature, and time. Chinese engineers have also contributed to the efficient pumping of in-tube concrete by solving the homogeneity problem during concrete preparation [8]. The properties of the concrete at the time of pumping are selected as the control objective to ensure homogeneity of the in-tube concrete.

Substantial shrinkage of the in-tube concrete may occur in the curing process due to a high dosage of elastomeric materials and a low water-to-binder ratio; this will result in de-bonding between the concrete and steel tubes. To address this challenge, Liu et al. [9,10] proposed a method for the precise compensation of varying degrees of shrinkage at different curing stages that employs composite expansive agents based on an analysis of the temporal variation in the concrete volume deformation. Modified azodiformamide is used to compensate for the plastic stage shrinkage, calcium-expanding materials are used to mitigate early-stage dry shrinkage, and high-activity magnesium oxide and medium-to-low-activity magnesium oxide are employed to address mid-stage and later-stage dry shrinkage. This method can control the expansion and contraction of in-tube concrete throughout the entire curing process.

The use of such new concrete admixtures, coupled with the vacuum-assisted pressure pumping technique, has effectively solved the longstanding challenges associated with concrete debonding and void formation within steel tubes, thereby optimizing the working performance of the steel–concrete composite arch ring in CFST arch bridges.

2.4. Design of a thrust abutment foundation on non-rocky stratums for large-span arch bridges

Large-span arch bridges generally offer significant technical and economic advantages. However, one notable challenge of this type of bridge lies in managing the substantial horizontal thrust imposed by the arch abutments. This necessitates a foundation with high resistance against thrust loads. Thus, it is customary to position the foundations of large-span thrust arch bridges on solid rock substrates. Nevertheless, the Pingnan Third Bridge has a unique geological condition, as it is located in a flat terrain. The southern bank has exposed bedrock, while the northern bank comprises a layer of clay with an underlying layer of pebble, each 15 m in depth. Judged by conventional standards, it is not advisable to construct a thrust arch bridge under such conditions. In the face of the contradiction between a seemingly unsuitable foundation and the high economic advantage of building a thrust arch bridge, an innovative design encompassing both superstructure optimization and abutment foundation improvement was proposed. This comprehensive design aims to reduce the loading demand and enhance the resistance of the abutment foundation, effectively

addressing the challenges associated with the abutment foundation construction of a large-span thrust arch bridge in a flat, plain terrain.

In the domain of superstructure optimization, the primary objective is to effectively mitigate the vertical force, horizontal thrust, and moment acting upon the arch foundation exerted by the permanent load. In addition, the centerline of the foundation is moved backward along the arch axis, thereby augmenting the moment generated by the permanent vertical force. This adjustment brings about an equilibrium between the moment generated by the horizontal thrust and the moment created by the permanent vertical force, consequently leading to a uniform distribution of the vertical stresses exerted upon the foundation and a notable reduction in its edge stress. Due to such superstructure optimization measures, the bearing capacity requirement for the abutment foundation of the Pingnan Third Bridge was reduced to less than 800 kPa, as shown in Table 3.

To enhance the foundation resistance, a novel composite foundation structure was proposed [11], as depicted in Fig. 7. It involves inserting a diaphragm wall deep into the bedrock and injecting cement slurry into the pebble layer enclosed by the diaphragm wall to enlarge the load-bearing capacity of the pebble layer. The abutment foundation is then directly situated atop the grouted pebble layer. The *in-situ* load test results revealed that the allowable bearing capacity of the grouted pebble layer increased by 53% compared with its pre-strengthened state. Furthermore, there was a noteworthy increase in the deformation modulus of the pebble layer. The measurement results showed that, 42 months after grouting, the settlement of the foundation was a mere 5.2 mm, which is far below the allowable settlement requirement of 30 mm. In addition, the pebble layer serves as a seismic damping layer [12].

The integrated foundation design technique described above extends the possibility of constructing large-span thrust arch bridges not only on rocky foundations but also on non-rocky substrates. This broadens their suitability from mountainous regions to flat terrain, significantly expanding the scope of application for thrust arch bridges.

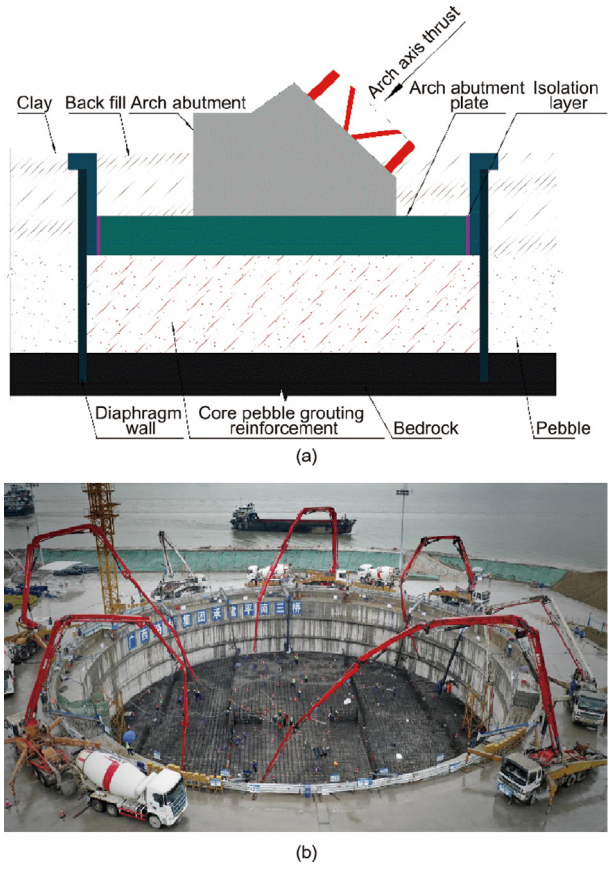

Fig. 7. New composite foundation of a diaphragm wall encapsulating the grouting-reinforced pebble layer for the abutment of a large-span thrust arch bridge. (a) Schematic diagram; (b) photograph during construction.

2.5. Optimization of large-scale temporary facilities for arch erection

Unlike the construction of large-span cable-stayed bridges or suspension bridges, the construction of large-span CFST arch bridges heavily relies on the utilization of large-scale temporary construction facilities. If the related expenses cannot be mitigated, the economic competitiveness of this bridge type will be lost.

At present, most large-span arch bridges are constructed by means of cable-stayed fastening-hanging cantilevered assembly with post-closure cable loosening. In this method, the suspension tower and buckle tower act as important temporary load-bearing structures within the erection system, and they constitute a large portion of the overall cost of temporary construction facilities. During the lifting of arch segments, horizontal forces are transmitted by the cables to the top of the suspension and buckle tower, which will induce lateral displacement to the tower. This lateral displacement leads to a coordinated deviation of the erected arch rib hanging on the tower, along with a substantial bending moment in the tower. The traditional approach to this problem involves either the separation of the suspension and buckle towers or setting a hinge between them to eliminate the influence of the suspension tower on the buckle tower; however, such treatments have a high cost. Alternatively, combining the two towers without a hinge necessitates enhancing the tower's horizontal stiffness and increasing the number of wind cables to reduce the tower top displacement. This approach falls within the domain of stiffness-based passive control; it also incurs a high cost, and the displacement control precision can be kept to only the decimeter level.

To address this challenge, an intelligent active control approach for tower displacement control was invented. This approach uses hydraulic jacks to actively exert force on the control cables so as to directly counteract the horizontal force exerted on the tower and thereby effectively minimize the tower top displacement.

Table 3
Checking results of the northern abutment foundation of the Pingnan Third Bridge.

Load case	Stress at front of the foundation bottom (kPa)	Stress at back of the foundation bottom (kPa)	Anti-sliding coefficient	Anti-overturning coefficient
1	647.7	694.2	1.41	61.88
2	720.2	606.9	1.54	24.76
2	755.8	582.8	1.53	16.52
4	615.9	715.4	1.43	28.38
Allowable criterion	$\leq$ 800.0	$\leq$ 800.0	1.30	1.50

Based on this approach, an intelligent control system was developed. The tower top displacement is real-time monitored by the Beidou Navigation Satellite System (BDS). An intelligent hydraulic jack system is employed to dynamically adjust the applied force to make the tower top promptly return to its original position [13], as shown in Fig. 8.

With the present active force control method, unlike the traditional passive stiffness control method, analysis shows that the tower only needs to meet the strength and stability requirements. In this way, the tower can be slenderized and the number of wind cables is reduced, saving cost on temporary construction facilities. Furthermore, horizontal displacement control at the tower top, which is realized through force adjustment, relies solely on the displacement measurement accuracy and system response rate. The control accuracy can be improved from the original decimeter level to the centimeter level. For example, in the case of the Pingnan Third Bridge, the tower is 202 m in height but has a narrow width of only 12 m in the longitudinal direction. Measurement and force adjustment were conducted at 6 s intervals. This active control approach ensures that the tower top position is maintained within a stable ±2 cm range, as depicted in Fig. 9. This technology has also been successfully applied in the construction of the Shuangpu Bridge on the new Chongqing–Hunan Expressway in China. This bridge is a two-span continuous CFST arch bridge with each span measuring 405 m. It effectively mitigates the offset stemming from a 4000 kN difference in cable tension due to the asynchronous erection of the two-span arch trusses, resulting in a notable reduction in the load borne by the central buckle tower.

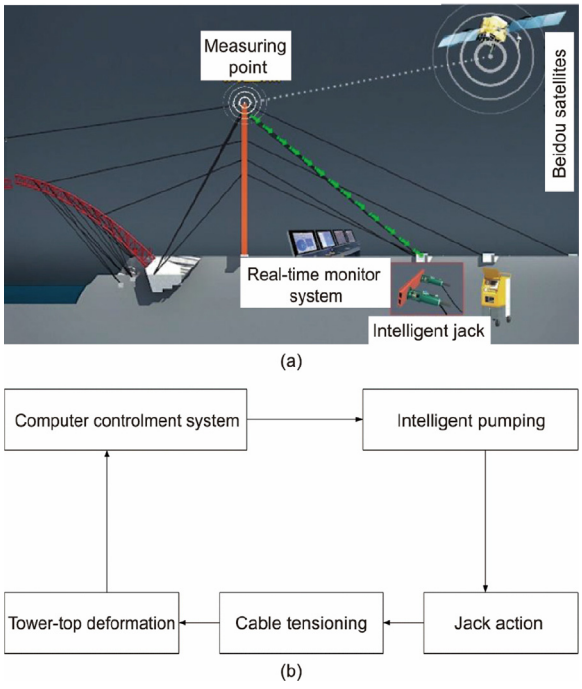

Fig. 8. Active force method for the horizontal displacement control of the suspension and buckle tower. (a) Control principle; (b) working procedure.

The buckle cables are another important part of the cable-stayed fastening-hanging cantilevered assembly system. The method employed for tensioning and removing buckle cables and adjusting the cable force has a strong influence on the construction safety, construction speed, arch alignment, and number of cables. The traditional cable tensioning method requires multiple tensioning iterations, which often leads to considerable variation in the arch alignment and cable force during the installation process. To address this problem, an arch rib alignment control method based on the impact matrix theory and the "optimized process" principle was proposed [14,15]. This method sets minimal vertical displacement and lateral deviation during the arch rib installation as the optimization objective, allowing an optimization model for calculating the buckle cable force and wind cable force during cable-stayed fastening-hanging cantilevered assembly to be established. The optimization model can be briefly expressed as follows:

$$\text{Find: } x = \{x_1, x_2, x_3, \ldots, x_n\} \tag{1}$$

$$\text{To minimize: } f(x) = \| \boldsymbol{u}_{\mathrm{h}}(x) - \boldsymbol{u}_{\mathrm{t}} \| \tag{2}$$

$$\text{Subject to: } \begin{cases} x_i \geq 0 \\ [\boldsymbol{u}_{\mathrm{n}}(x) - \boldsymbol{u}_{\mathrm{t}}]^2 \leq \Delta u^2 \end{cases} \tag{3}$$

where x_i is the initial tension force of the ith buckle cable, i = 1,2,. . ., n; $\boldsymbol{u}_{\mathrm{t}}$ and $\boldsymbol{u}_{\mathrm{n}}(x)$ represent the target and real displacement vector of the arch axis after bridge closure, respectively; $\boldsymbol{u}_{\mathrm{h}}(x)$ denotes the pre-elevation of the arch axis; and Δu is the displacement deviation threshold.

Through this optimization model, the initial force for each group of buckle cables and the initial elevation and axial deviation of each cantilever segment are obtained. Thus, a one-time tensioning operation is realized for all buckle cables without subsequent adjustment, which minimizes fluctuation in cable forces. Since the need for the number of buckle cables is governed by the maximum cable force principle during construction, it also leads to a substantial decrease of 15%–20% in the consumption of cables. Fig. 10 provides a comparison between the measured and predicted vertical displacement evolution curve of the No. 5 segment on the downstream side of the Xialao Bank of the Tian'e

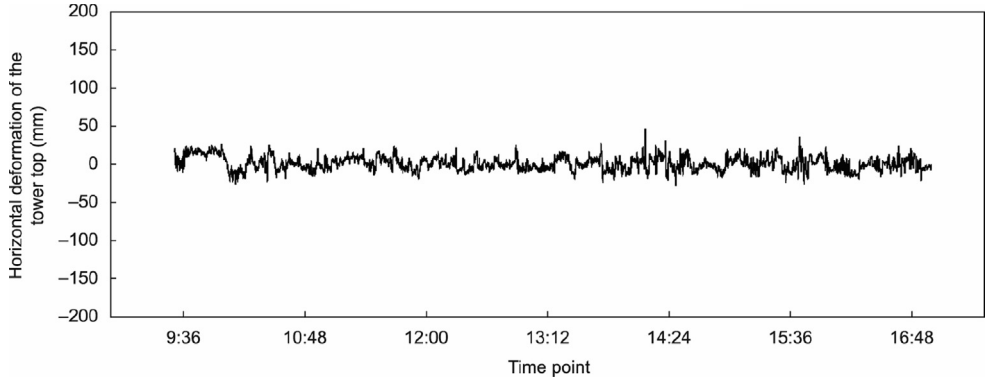

Fig. 9. Horizontal displacement evolution of the southern tower of the Pingnan Third Bridge during the installation of the No. 4 steel arch truss segment.

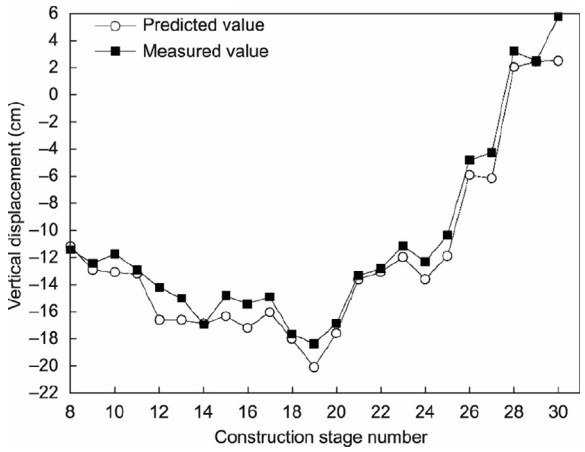

Fig. 10. Comparison between the measured vertical displacements of the No. 5 segment of the Tian'e Longtan Bridge during the steel tube arch truss erection under the proposed one-time cable tensioning method, with the predicted values.

Longtan Bridge during the steel tube arch truss erection using this one-time cable tensioning method.

For the post-closure cable dismantling, an expedited cable-removal method was introduced. Using this method, cables are dismantled alternately between the arch springing to the one-quarter span and from the one-quarter span to the arch crown. This approach achieves a one-shot removal of all buckle cables, thereby significantly reducing the construction duration and risk [16].

In summary, Chinese engineers have conducted extensive research and practice in the realm of large-span CFST arch bridges and their construction. Pioneering techniques have been introduced to address related challenges. Cable-stayed fastening-hanging cantilevered assembly realizes large-span arch erection without external support. The introduction of vacuum-assisted multistage continuous pumping and novel non-shrinkage materials for in-tube concrete has effectively mitigated the longstanding problems of in-tube concrete delamination and void formation, thereby ensuring the structural integrity of CFST arch ribs. A new bridge abutment foundation on non-rocky stratums has been developed to enhance the load-bearing capacity of the foundation; this resolves the difficulties associated with the construction of large-span thrust arch bridges in regions lacking a solid rock foundation and thereby expands the application of such arch bridges. An active force control method for tower displacement regulation, as an alternative to the traditional stiffness control method, has been introduced, resulting in high control accuracy and significant reduction in the size of suspension and buckle towers. Research efforts have also been paid to the fabrication of arch segments and the tensioning of buckle cables, leading to substantial cost reduction and enhanced safety in arch truss erection. All of these innovations have been successfully implemented in the construction of the Pingnan Third Bridge. Some research findings and practices associated with CFST arch bridges have been incorporated into the national and industrial standards of China, including GB 50923-2013 [17] and JTG/T D6-2015 [18].

3. SRC arch bridges

Like the CFST arch bridge, the concrete arch bridge exhibits excellent structural performance in terms of mechanics. However, it has a considerable mass. More specifically, a concrete arch is 5–10 times heavier than the beam of a cable-stayed or suspension bridge with the same length. Moreover, the curved configuration of the arch makes its erection laborious and expensive. To facilitate the arch erection of concrete arch bridges, Austrian engineer Josef Melan introduced the stiff skeleton method in 1898. In this method, a lightweight steel arch skeleton is erected first. A formwork is suspended from the skeleton, and encasing concrete is then poured to form an integral arch. The steel skeleton generally weighs one-tenth or less of the total weight of the encasing concrete. Concrete arch bridges constructed using such a method are called SRC arch bridges.

Later, Chinese engineers improved this method by replacing the steel skeleton with a CFST skeleton. A formwork is suspended from the CFST skeleton, and the pouring of the encasing concrete is conducted layer by layer, platform by platform, and segment by segment. During such a pouring procedure, special attention must be dedicated to crack prevention, given the big differences in the curing times between adjacent concrete layers. Taking the Tian'e Longtan Bridge as an example, a two-month discrepancy exists in the curing periods between the bottom layer and the web layer concrete of the arch rib. If there were no appropriate regulation measures, the web layer of concrete would have a maximum longitudinal tensile stress of 3.7 MPa, since its shrinkage is constrained by the bottom layer of concrete. In the practical project, expansion agents containing retarding components were added to the web concrete to induce volume expansion, thereby eliminating the tensile stress, as illustrated in Fig. 11. Since the difference in the concrete curing time between segments within one layer is less than ten days, appropriate crack control measures can be taken, as with construction joints. The installation method for the CFST skeleton is almost the same as that used for the CFST arch, with the exception that H-section steel is often utilized in the web members of the CFST skeleton to facilitate its adhesion with the encasing concrete.

As of the year 2024, the global count of concrete arch bridges with a span exceeding 200 m is 67, of which 20 are SRC arch bridges. Among the 20 concrete arch bridges with a span larger than 300 m, 11 bridges are SRC arch bridges and all of them are in China, as listed in Table 4. Furthermore, all five concrete arch bridges with a span greater than 400 m are SRC arch bridges. The Beipan River Bridge on the Shanghai–Kunming High Speed Railway was completed in 2016. Its span of 445.0 m set the world record for concrete arch bridges when it was completed. Recently, this world record has been elevated to the greater length of 600.0 m by the Tian'e Longtan Bridge.

China's consistent ascent to new heights in the realm of SRC arch bridges can mainly be attributed to two technological advancements. The first of these advancements is the replacement of the steel stiff skeleton with the CFST stiff skeleton, which achieves a 50% reduction in steel, resulting in significant savings

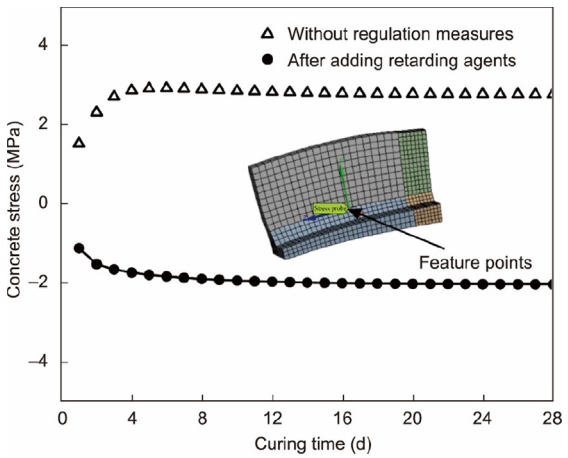

Fig. 11. Constrained shrinkage stress in the web concrete of the arch rib of the Tian'e Longtan Bridge.

Table 4
List of concrete arch bridges with spans greater than 300 m.

No.	Bridge	Main span (m)	Bridge type	Construction method of the arch	Year of completion
1	Tian'e Longtan Bridge	600.0	Reinforced concrete deck arch bridge	Stiff skeleton method	2024
2	Xining River Bridge	510.0	Reinforced concrete deck arch bridge	Stiff skeleton method	Under construction
3	Shanghai–Kunming High Speed Railway Beipan River Bridge	445.0	Reinforced concrete deck arch bridge	Stiff skeleton method	2016
4	Wanzhou Yangtze River Bridge	420.0	Reinforced concrete deck arch bridge	Stiff skeleton method	1997
5	Nanning–Kunming High Speed Railway Nanpan River Bridge	416.0	Reinforced concrete deck arch bridge	Stiff skeleton method	2016
6	Krk Bridge	390.0	Reinforced concrete deck arch bridge	Cantilevered assembly in form of truss	1980
7	Almonte Railway Bridge	384.0	Reinforced concrete deck arch bridge	Hanging-basket-assisted *in situ* casting	2016
8	Leshan–Xichang Highway Suba Bridge	370.5	Reinforced concrete deck arch bridge	Stiff skeleton method	Under construction
9	Yelang River Bridge	370.0	X-style reinforced concrete deck arch bridge	Stiff skeleton method	2018
10	Zhaohua Jialing River Bridge	364.0	Reinforced concrete deck arch bridge	Stiff skeleton method	2012
11	Dali–Ruili Railway Lantsang Bridge	342.0	Reinforced concrete deck arch bridge	Two-stage vertical rotation	2022
12	Zhengzhou–Chongqing Railway Meixi River Bridge	340.0	X-style reinforced concrete deck arch bridge	Stiff skeleton method	2022
13	Luzhou–Gulin Highway Shuiluo River Bridge	335.0	Reinforced concrete deck arch bridge	Hanging-basket-assisted *in situ* casting	Under construction
14	Jiangjie River Bridge	330.0	Truss-type prestressed concrete deck arch bridge	Cantilevered assembly	1995
15	Tajo Railway Bridge	324.0	Reinforced concrete deck arch bridge	Hanging-basket-assisted *in situ* casting	2019
16	Mike O'Callaghan–Pat Tillman Memorial Bridge	323.0	Reinforced concrete deck arch bridge	Hanging-basket-assisted *in situ* casting	2010
17	Wen'an—Machangpin Railway Wujiang River Bridge	320.0	Reinforced concrete deck arch bridge	Cantilevered assembly	Under construction
18	Yongning Yong River Bridge	312.0	Half-through concrete arch bridge	Stiff skeleton method	1996
19	Gladesville Bridge	304.8	Reinforced concrete deck arch bridge	Assembly on bracket	1964
20	Guansheng Qujiang River Bridge	300.0	Half-through concrete arch bridge	Stiff skeleton method	2019

in material cost and a reduction in the lifting demand. The remarkable achievements in CFST arch bridge construction in China have also indirectly propelled the development of SRC arch bridges with a CFST stiff skeleton. The second advancement is the technique for the temporary stress control and permanent stress reduction of the CFST skeleton during the pouring of encasing concrete. The idea of replacing the steel skeleton with a CFST skeleton was originally proposed by the Sichuan Highway Planning, Survey, Design, and Research Institute, Ltd. during the design of the Wanzhou Yangtze River Bridge, which has a span of 420 m. The technique for the temporary stress control and permanent stress reduction of the CFST skeleton was first used by the Guangxi Road and Bridge Engineering Group Corporation on the Yongning Yong River Bridge, which has a span of 312 m. Details on these two technological breakthroughs can be found in Ref. [1].

For large-span concrete arch bridges built outside China, the predominant method employed for the arch rib erection is *in situ* casting on hanging baskets. Of the 26 concrete arch bridges with a span exceeding 200 m built outside China, 20 employed the hanging-basket-assisted casting approach. Among these, the Almonte Bridge in Spain, which was completed in 2016, stands out with its largest span of 384 m. In China, within the 41 concrete arch bridges with a span larger than 200 m, only nine used the hanging-basket-assisted casting method for arch erection. Within these nine bridges, the Shuiluo River Bridge situated on the Luzhou–Gulin Expressway has the largest span of 335 m. A comparison between the hanging-basket-assisted casting method and the stiff skeleton method in terms of economy can be found in a paper published by Zheng and Wang [1].

In the rest of this section, scientific and technological breakthroughs in large-span SRC arch bridges are introduced using the world's largest-span arch bridge, the Tian'e Longtan Bridge, as an example.

3.1. Overview of the Tian'e Longtan Bridge

The Tian'e Longtan Bridge is located in the reservoir area of Tian'e County, Guangxi Zhuang Autonomous Region, China, and it is a key project on the Nandan–Tian'e Expressway in Guangxi. The river channel under the bridge is in a U shape, with steep mountains on both sides. The river is about 600 m wide and 160 m deep, and there is an annual maximum water level drop of 45 m.

The total length of the bridge is 2488.55 m. Its main span is an SRC deck-type twin-ribbed arch bridge. Each arch rib has a catenary profile, featuring an effective span of 600 m, an effective rise of 125 m, a rise-to-span ratio of 1/4.8, and an arch axis coefficient of 1.9. The arch ribs have a concrete box section of uniform width and variable height, with a box section height of 12 m at the arch springing and 8 m at the arch crown. The box section is 6.5 m in width. Two arch ribs are longitudinally aligned, maintaining a center-to-center spacing of 16.5 m. At all positions below the arch columns (40 m apart), concrete box-type transverse connection members are installed, for a total of 13 connection members along the arch. Both the arch ribs and the transverse connection members are constructed with high-performance concrete at a strength grade of C60 (concrete with a standard cubic compressive strength of 60 MPa). The arch ribs adopt a CFST skeleton. The overall layout of the bridge is shown in Fig. 12.

The stiff skeleton of each arch rib is an arch truss with four CFST chords. The steel tubes of both the upper and lower chords have a strength grade of Q420qD (specified by the Chinese code [19], in which Q denotes the yield strength of the steel, 420 indicates that the minimum yield strength of the steel should not be less than 420 MPa, q indicates that the steel is specifically used for bridges, D represents a quality level of the steel), with a diameter of 900 mm and a wall thickness ranging from 30 to 35 mm. The

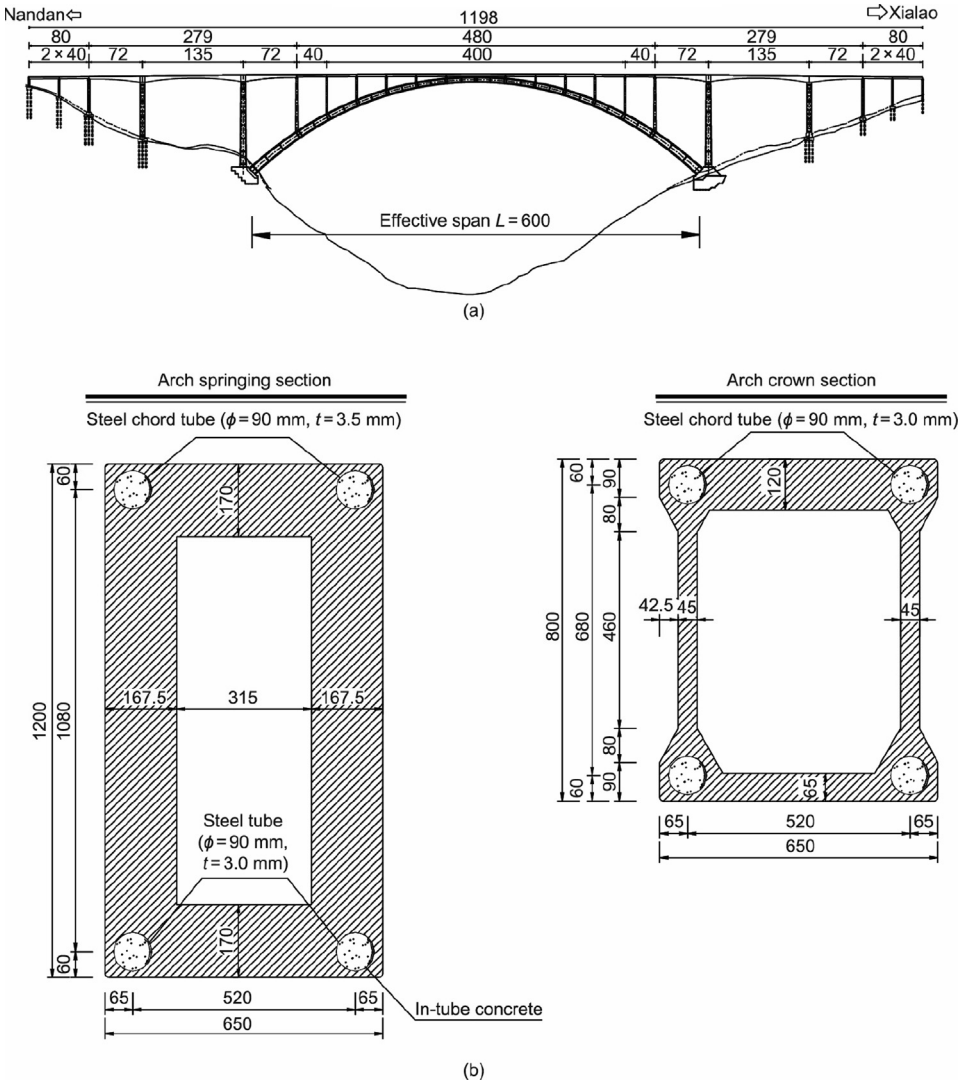

Fig. 12. General layout of the structural design of the Tian'e Longtan Bridge. (a) Overall elevation arrangement (unit: m); (b) section diagram of the arch ribs (unit: cm). ϕ: diameter of steel chord tube; t: thickness of steel chord tube.

diagonal braces and transverse ties connecting the chord tubes are welded angle steel, and are affixed to the chord tubes via node plates. The chord tubes between adjacent arch truss segments are joined with flange bolts outside the tube, followed by the external welding of the tubes. The chord tubes are filled with C80 (concrete with a standard cubic compressive strength of 80 MPa) self-compacting slightly expansive concrete. A cross-sectional view of the stiff skeleton is shown in Fig. 13.

The steel tube arch trusses of the CFST skeleton were erected using the cable-stayed fastening-hanging cantilevered assembly method, as shown in Fig. 14. Each steel arch truss was divided into 24 segments, with the heaviest one weighing 169 metric tons. The encasing concrete was poured layer by layer and segment by segment. The concrete encasing each arch rib was vertically divided into three layers: the bottom plate layer, the web plate layer, and the top plate layer. Each layer was symmetrically poured on eight working platforms along the arch axis. Eight pressure pumps were employed concurrently, allowing for simultaneous concrete pouring on four working platforms. This procedure was iterated 36 times to complete the pouring of the encasing concrete for the two arch ribs, as depicted in Fig. 15. A total of 28 100 m^3 of encasing concrete was poured. The main construction progress of the Tian'e Longtan Bridge is summarized in Table 5. Fig. 16 presents the deflection and stress evolution curves of the bridge during construction, which show good agreement between the measured and predicted values. The bridge has now been completed and is open to traffic. Fig. 17 provides a glimpse of the bridge's appearance as of February 2024.

The main span of the Tian'e Longtan Bridge is 600 m long, establishing a new world record for concrete arch bridges. This surpasses the previous record by 155 m, which is equivalent to the cumulative increase in the span of concrete arch bridges over the past century. Undoubtedly, this project carried substantial construction risks. Nevertheless, concrete arch bridges such as the Tian'e Longtan Bridge offer notable advantages, including high stiffness, long durability, and minimal maintenance requirements. In addition, construction of such a bridge saves approximately 125 million CNY compared with a cable-stayed bridge with the same span length, making it a highly economically viable choice. However, despite the author's prior experiences in the construction of concrete arch bridges with spans of 300 and 400 m, the construction of a concrete arch bridge with a 600 m span presented unprecedented challenges to the author due to the absence of previous instances of building such a long arch bridge anywhere in the world. In the next section, the technical challenges of and corresponding solutions employed in the construction of

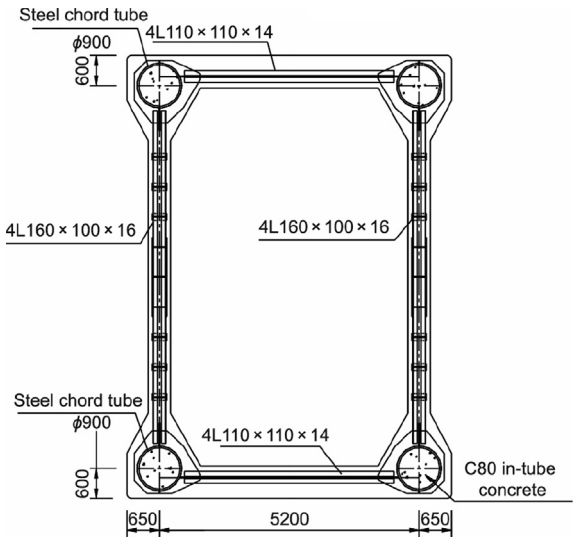

Fig. 13. Section diagram of the steel stiff skeleton of the Tian'e Longtan Bridge (unit: mm). $aLb \times c \times d$: a denotes the number of the individual welded angle steel member; L denotes "L" type welded angle steel member; b, c, and d denotes the sectional length, width, and thickness of the individual welded angle steel member.

super-large-span SRC arch bridges will be elaborated, with the Tian'e Longtan Bridge as a case study.

3.2. Stiffness design of the CFST skeleton

During the construction of SRC arch bridges with a CFST skeleton, the CFST skeleton serves as a crucial support structure; a highly stiffened skeleton is preferred because of its role in mitigating risks in arch construction. Nevertheless, the presence of a highly stiffened skeleton inevitably leads to greater difficulties in the construction of the skeleton itself, while also diminishing the economic advantage of the bridge. Therefore, the selection of an appropriate stiffness for the CFST skeleton is of great importance. The ratio of the mass of the steel tube truss in the CFST skeleton to the mass of the encasing concrete is generally utilized to measure the skeleton stiffness. Although this ratio provides a straightforward and intuitive index, it is not precise enough, because the ratio should be increased with an extension of the span length. According to the eight completed SRC arch bridges, this ratio falls between 1/13.2 and 1/15, as detailed in Table 6. In the case of the Tian'e Longtan Bridge, the steel tube truss of the CFST skeleton has a weight of 8150 metric tons, while the encasing concrete volume amounts to 28 100 m^3, yielding a mass ratio of 1/8.6. Although this ratio is apparently higher than that of the other completed SRC bridges, the stiff skeleton still could not independently support the substantial weight of the 70 000 metric tons of encasing concrete for the Tian'e Longtan Bridge, necessitating a multi-layer pouring of the encasing concrete. This situation differs from that of a CFST arch bridge. For example, the Pingnan Third Bridge has a 560 m span, and the 8440-tonne steel arch truss can fully support 20 000 metric tons of in-tube concrete, allowing for one-time pouring of the in-tube concrete.

The pouring of the encasing concrete for each arch rib of the Tian'e Longtan Bridge was divided into three layers: the bottom plate layer, web plate layer, and top plate layer, with the corresponding concrete volumes of 8800, 11 000, and 8300 m^3, respectively. Each layer comprised eight working platforms, and each working platform underwent six casting cycles. For each cycle, four working platforms were simultaneously cast. Each layer was completed with 12 cycles of casting.

It is noteworthy that the stress and deflection in the stiff skeleton increased very rapidly during the pouring of the in-tube concrete and the encasing concrete at the bottom layer. In these two phases, the mid-span deflection of the arch ribs had a substantial increase of 698 mm, which constituted 60% of the overall deflection of 1156 mm during the whole encasing concrete pouring process. This deflection is also 8.3 times greater than the combined deflection during the concrete pouring of the web and top layers. The stress in the upper steel tube chords of the stiff skeleton increased by 210 MPa, accounting for 61% of the cumulative stress of 340 MPa for the whole encasing concrete construction process. This stress increment is also 3.7 times higher than that during the concrete pouring in the web and top layers. Despite the fact that the combined mass of the encasing concrete in the web and top layers was 1.6 times heavier than the combined mass of the in-tube concrete and the encasing concrete in the bottom layer, it is important to note that the load-bearing structures during the pouring of the in-tube concrete and the bottom layer of encasing concrete were the steel tube truss and the CFST arch truss, which had relatively low rigidity. The stiffness of the steel skeleton was therefore primarily determined by these two construction phases. Subsequently, the stiffness of the CFST skeleton significantly increased upon its integration with the bottom layer of encasing concrete. As a result, the rate of increase of the deflection and stress in the arch ribs slowed down in the subsequent construction phases. However, it should be noted that, before the upper steel tube chords were covered by the top layer of encasing concrete, the maximum stress of the chord was 340 MPa, nearly reaching the allowable stress of 360 MPa for Q420qD steel specified by the Chinese design code for railway steel bridges [19]. Moreover, during the pouring of the encasing concrete at the bottom layer, the CFST skeleton of the Tian'e Longtan Bridge effectively withstood the effect of a 3250 kN loading difference between the two halves of the arch rib arising from a concrete pumping pipe blockage. Following the completion of the pouring of the encasing concrete, the CFST skeleton was embedded in the encasing concrete, thereby enhancing the strength and ductility

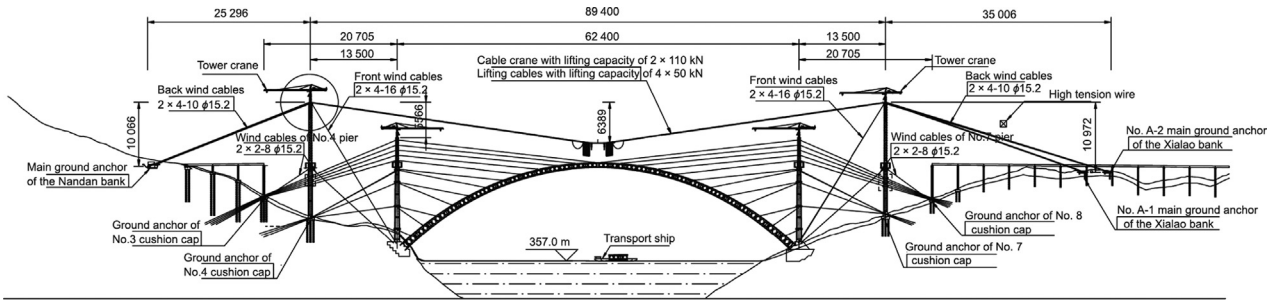

Fig. 14. Cable-stayed fastening-hanging cantilevered assembly system for the steel arch truss erection of the Tian'e Longtan Bridge (unit: cm). $l \times m$-n: l denotes the number of individual wind cables; m denotes the number of steel strand bundle in each wind cable; n denotes the number of steel strand in each steel strand bundle.

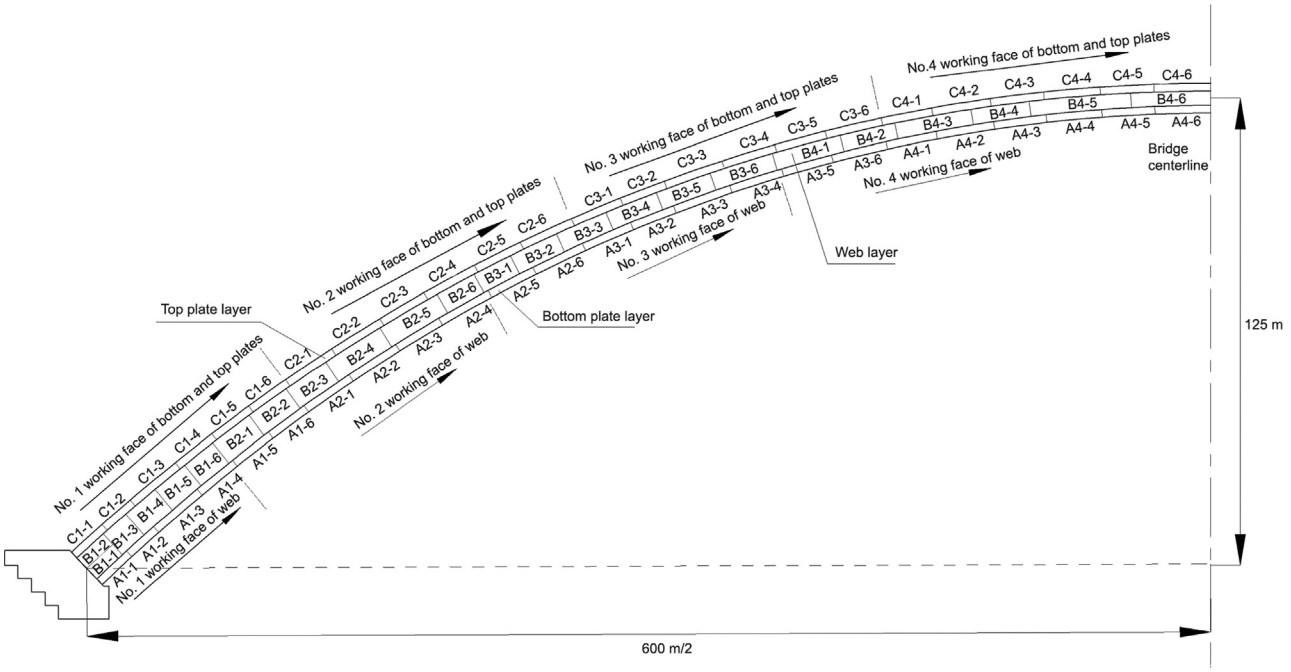

Fig. 15. General layout of the layer, segment, and working face settings for the encasing concrete pouring of the arch ribs of the Tian'e Longtan Bridge. The symbol labeled on the arch such as "B1-2" represents the pouring order of the encasing concrete segments. The first letter represents the identifier of the layer that the segment stands on, and A, B, and C denote the bottom plate layer, web plate layer, and top plate layer, respectively; the second number represents the order of the working face (platform) within each layer; the third number represents the order of the encasing cycle within each working face.

Table 5
Overview of the construction time of the Tian'e Longtan Bridge.

Time (month/day/year)	Key construction phase	Duration (d)
2/28/2022	Erection of the first steel tube stiff skeleton segment	100
6/6/2022	Steel tube stiff skeleton closure	
7/29/2022	In-tube concrete filling of the first two chord tubes of the stiff skeleton	10
8/9/2022	In-tube concrete filling of the last two chord tubes of the stiff skeleton	
9/15/2022	First pouring of the encasing concrete in bottom plates	54
11/8/2022	Final pouring of the encasing concrete in bottom plates	
11/26/2022	First pouring of the encasing concrete in webs	80
2/17/2023	Final pouring of the encasing concrete in webs	
3/10/2023	First pouring of the encasing concrete in top plates	50
4/30/2023	Final pouring of the encasing concrete in top plates	
4/15/2023	Start of construction of spandrel columns	138
8/31/2023	Completion of construction of spandrel columns	
10/5/2023	Start of traffic beam installation	36
11/9/2023	Completion of traffic beam installation	
12/2/2023	Start of bridge deck paving	24
12/26/2023	Completion of deck paving	

of the SRC arch ribs. Evidently, the stiffness selected for the CFST skeleton of the Tian'e Longtan Bridge is appropriate.

The analysis above shows that the supporting function of the stiff skeleton is one of the key matters to be considered when determining the appropriate stiffness of the CFST skeleton of an SRC arch bridge. In particular, special attention should be directed to the stress and deformation of the stiff skeleton that occur during the pouring of the first layer of encasing concrete.

3.3. Pouring of the encasing concrete of the arch ribs

In China, most concrete arch bridges are constructed using the stiff skeleton method, in which the arch rib formation is a self-supporting process. However, one of the prevailing approaches outside China is a combination of hanging-basket-assisted casting with the stiff skeleton method. In this approach, the two side segments of the arch rib are first cast in the full section on the support of hanging baskets; then, the middle segment is constructed using the stiff skeleton method. Temporary hinges are positioned between the side and middle segments, as in the case of the Teishicho Bridge in Japan, with a 145 m span [20]. However, as the bridge span length increases, the intricacies of the hinge fabrication, installation, and construction also escalate. Consequently, the maximum span length of an SRC arch bridge constructed using this approach is limited to 260 m.

In China, the construction approach is quite different. It involves the erection of a CFST skeleton, followed by the pouring of encasing concrete layer by layer and segment by segment. Once the encasing concrete in the first layer (i.e., the bottom plate layer) is poured and attains the required strength, it forms a steel–concrete composite structure with the CFST skeleton, which significantly increases the load-bearing capacity and stiffness of the arch.

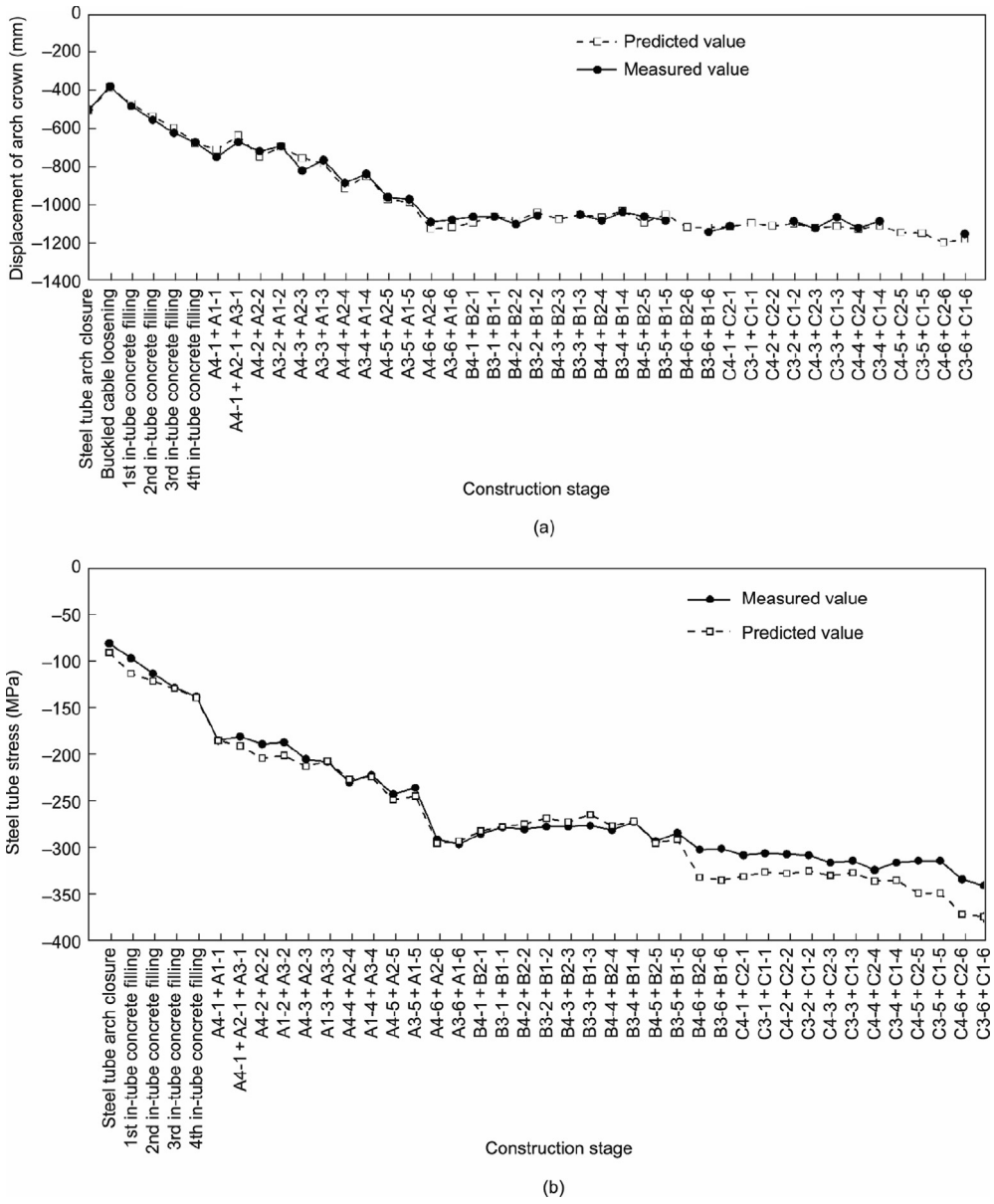

Fig. 16. Structural response evolution curves of the Tian'e Longtan Bridge during the construction process. (a) Displacement of the arch crown; (b) stress of the upper steel chord tube at the arch springing section.

Subsequent layers of encasing concrete are cast in a similar manner, incrementally enhancing the load-bearing capacity and stiffness of the arch until the whole arch rib is formed. Evidently, the method adopted in China is much simpler and offers a more rapid enhancement of the load-bearing capacity and stiffness of the arch ribs during the self-supporting process. This is also the underlying reason why China can consistently increase the world record for concrete arch bridge spans, from the 445 m of the Beipan River Bridge on the Shanghai–Kunming High Speed Railway in 2016 to the 600 m of the Tian'e Longtan Bridge this year. However, it is imperative to note that the mass of the encasing concrete is 9–15 times greater than that of the steel arch truss of the CFST skeleton, rendering the casting of the encasing concrete the most critical and perilous phase in the construction of an SRC arch bridge. This phase entails long and repeated loading on the arch. Once failure occurs during concrete pouring, there is hardly any effective remedial measure. In addition, as the encasing concrete is poured in a multilayer, multi-working platform, and multi-cycle manner, both the CFST skeleton and the hardened encasing concrete acquire time-dependent transient stresses. These time-dependent transient stresses might exceed the material strength, so stringent

Fig. 17. Recent photograph of the Tian'e Longtan Bridge (taken in February 2024).

Table 6
Material consumption information of SRC arch bridges with spans greater than 300 m.

No.	Bridge	Main span (m)	Steel consumption of stiff skeleton (t)	Encasing concrete consumption (m^3)	Weight ratio of steel in stiff skeleton to encasing concrete
1	Shanghai–Kunming High Speed Railway Beipan River Bridge	445	4709	26 500	1/14.2
2	Nanning–Kunming High Speed Railway Nanpan River Bridge	416	4011	24 000	1/15.0
3	Chongqing–Guizhou Railway Yelang River Bridge	370	5531	29 370	1/13.2
4	Dali–Ruili Railway Lantsang Bridge	342	5520	16 800	1/7.6
5	Zhengzhou–Chongqing Railway Meixi River Bridge	340	2545	14 210	1/13.9
6	Zhaohua Jialing River Bridge	364	1866	11 130	1/14.9
7	Wanzhou Yangtze River Bridge	420	2091	11 000	1/13.2
8	Yongning Yong River Bridge	312	852	4 816	1/14.7
9	Tian'e Longtan Bridge	600	8150	28 100	1/8.6

control measures must be taken, such as proper division of the casting layers and optimal setting of the working platforms. Once the encasing concrete attains the required strength and stiffness, it assumes the role of a primary load-bearing component. Meanwhile, as the CFST skeleton is embedded within the concrete, it further enhances the load-bearing capacity and ductility of the arch rib.

During the construction of the Tian'e Longtan Bridge, the total volume of the concrete encasing the arch ribs amounted to 28 100 m^3. The pouring of the encasing concrete was divided into three layers and eight working platforms. Concrete was simultaneously poured on four working platforms. The pouring procedure for arch ribs was completed through a cumulative 36 cycles. To ensure the lateral stability of the main arch structure during the pouring of the encasing concrete, permanent transverse connections in the form of reinforced concrete box girders were installed between the arch ribs at intervals of 40 m along the arch axis. In addition, 20 temporary transverse X-shaped steel tube braces were positioned between the upper chord tubes of the arch ribs, and then removed after the pouring of the encasing concrete of the bottom and web layers. Fig. 18 shows a curve depicting the change in the elastic stability coefficient of the arch ribs during the construction phase.

Each cycle of concrete pouring consumed approximately 800 m^3 of concrete and lasted for 7–10 h. To facilitate this process, eight pumps were simultaneously employed to ensure a concurrent supply of concrete to the four working platforms. No cables for load adjustment were needed in the pouring process. There were no transient tensile stresses in the in-tube concrete, and the transient tensile stress in the encasing concrete remained below 1 MPa. This effective control of transient stresses can be attributed to the deployment of eight pumps, which enabled simultaneous concrete pouring across four working platforms, unlike the sequential pouring on each working platform by a single pump on both sides of the arch. This innovative procedure was based on previous research findings [1]. More specifically, structural analysis indicates that the arch springing sections endure the greatest forces during the pouring of the encasing concrete—particularly the negative moment. Moreover, an influence line analysis indicates that the weight of the encasing concrete from the arch springing to the one-quarter span causes a negative moment in the arch springing section, while the weight of encasing concrete from the one-quarter span to the arch crown induces positive moment in the arch springing section. Therefore, a setting of four or eight working platforms is preferred over six working platforms, since casting can be conducted symmetrically in both the positive- and negative-moment-influencing regions of the arch springing section on one or two working platforms at the same time. In this way, a moment balance at the arch springing section can easily be obtained.

3.4. Development of the encasing concrete materials

During the curing process of the encasing concrete in the arch ribs of an SRC arch bridge, the concrete continuously undergoes substantial multidirectional constraints from the stiff skeleton, which is likely to induce restrained shrinkage cracks in the concrete. The traditional solution to this problem includes increasing the quantity of reinforcing steel and adding fibers into the concrete. However, increasing the quantity of reinforcing steel has almost no effect on the shrinkage cracking resistance of the encasing concrete. It is true that the introduction of fibers can offer a measure of crack resistance to the concrete; however, polymer fibers are easily aggregated and intermingled due to the long pumping distance of the encasing concrete, bringing new

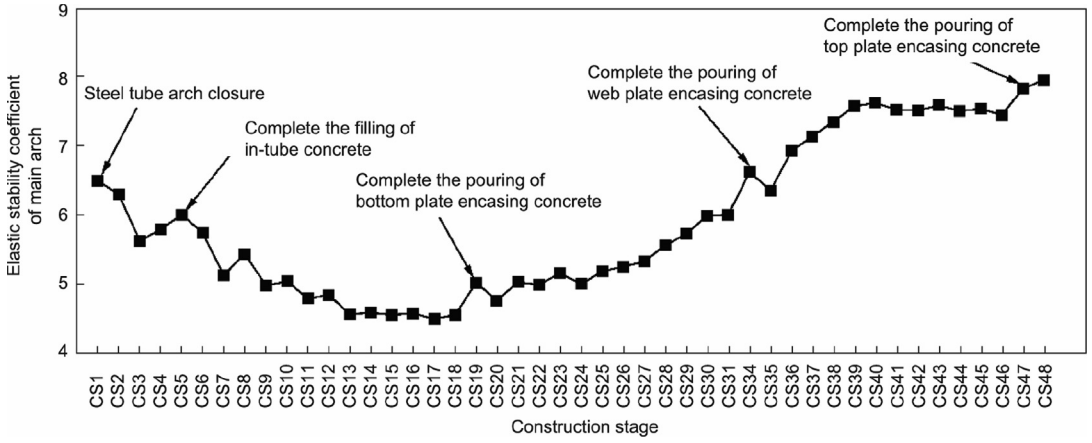

Fig. 18. Evolution curve of the overall elastic stability coefficient of the main arch of the Tian'e Longtan Bridge during the construction process. CS: construction stage.

challenges to the regulation of the encasing concrete. In fact, the most efficacious approach to mitigating shrinkage cracking of the encasing concrete is the incorporation of well-designed expansive agents to counteract concrete shrinkage. With regard to the workability control of concrete, one of the key considerations is to ensure the concrete's homogeneity. To this end, a real-time adjustment of the concrete's workability at the pumping site is required to ensure the stability and homogeneity of the concrete before it is poured into the formwork.

While expansive agents are utilized to prevent shrinkage cracking, expansion cracking in the surface of the encasing concrete should be emphasized. The underlying mechanism is rooted in the fact that the encasing concrete undergoes significant and uneven volumetric deformation at its surface, primarily due to intricate internal constraints and prolonged expansive deformation. For example, in a full-scale 12 m arch segment model test of the Tian'e Longtan Bridge, an expansion agent incorporating magnesia oxide was employed. While no early-stage cracks were observed, the first crack appeared in the concrete approximately three months after casting. More new cracks then occurred 262 days after casting. The analysis results showed that these cracks were mainly caused by the accumulated tensile stress resulting from continuous expansion of the concrete. To be specific, the external concrete of the full-scale arch segment model was directly in contact with the curing water, so its hydration occurred earlier than that of the internal concrete. After several months of operation, the external concrete was almost completely hydrated, such that no continuous volume deformation would occur, while the internal concrete still underwent an expansion trend due to the continuous effect of the anaphase expansion agents (i.e., the light burned magnesium oxide). This uneven volume deformation between the external and internal concrete continuously caused unrecoverable and cumulative tensile stress in the external concrete, finally resulting in the occurrence of cracking. In contrast, it is well known that concrete cracking due to other mechanisms, such as hydration heat and dry shrinkage, naturally occurs in the early stage. Consequently, it is imperative to consider the hydration process of the binding materials when selecting expansion agents. A well-designed expansive agent should enable appropriate early expansion for shrinkage compensation and avoid volumetric deformation during the later stages, as shown in Fig. 19.

In addition to shrinkage compensation, temperature and humidity difference control within and outside of the concrete is also an indispensable prerequisite for mitigating the temperature stress and drying shrinkage stress of the encasing concrete of the arch ribs. Thus, rigorous temperature control measures should be taken in different concrete-related operations, including preparation, transportation, and pumping. During the curing phase, external covering was applied to reduce the temperature difference between the inside and surface of the concrete. Furthermore, continuous spraying and misting served to maintain the moisture level, thereby mitigating the risk of surface drying. These multifaceted measures resulted in good casting quality and high cracking resilience of the encasing concrete in the arch ribs of the Tian'e Longtan Bridge. Overall, it can be seen that the admixture selection principles and casting techniques employed on the Tian'e Longtan Bridge hold broad significance within the domain of SRC arch bridge construction.

3.5. Stress reduction of encasing concrete

In a large-span SRC arch bridge, the stress in the arch rib caused by the permanent load constitutes a substantial proportion—ranging from 91.7% to 96.6%—of the total stress caused by the combined permanent and live loads, as outlined in Table 7. The weight of the arch rib accounts for approximately 60% of the total weight

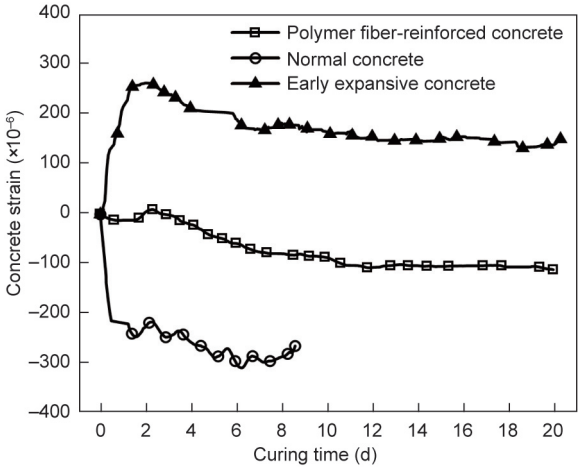

Fig. 19. Evolution curves of free strain for concrete with different mix proportions.

of the whole superstructure of an SRC arch bridge, as indicated in Table 8. Moreover, as illustrated in Section 3.2, the stiffness and material requirements of the CFST skeleton largely depend on the weight of the encasing concrete. Therefore, it can be concluded that the primary avenue for reducing the concrete stress of an SRC arch bridge hinges on reducing the weight of the arch ribs, especially that of the encasing concrete. To this end, in the arch rib design of the Tian'e Longtan Bridge, the traditional design of a single rib configuration was replaced by a twin rib configuration, as illustrated in Fig. 20. The single rib configuration has a one-box section with three cells, while the twin rib configuration has a one-cell box section. Consequently, compared with the traditional single rib design, the top and bottom plates of the middle cell of the new design were eliminated. Moreover, a varied thickness along the arch axis was adopted for the bottom plates, web plates, and steel tubes of the CFST skeleton. Through the above measures, the total volume of the encasing concrete for the arch ribs of the Tian'e Longtan Bridge was reduced from the originally designed 36 000 to 28 100 m^3.

Regarding the structures above the arch, optimization measures were also conducted. It is known that the region from the arch springing to the one-quarter span lies within the negative range of the influence line of the arch springing moment, while the region from the one-quarter span to the arch crown falls within the positive range. Therefore, the traffic beams should maintain a relatively lightweight design above the region from the arch springing to the one-quarter span, while avoiding excessive lightness from the one-quarter span to the arch crown. To this end, a prestressed concrete continuous rigid frame structure was employed for the traffic beam near the arch springing to avoid the need for high spandrel columns in the Tian'e Longtan Bridge. For the remaining region, conventional prestressed concrete T-type beams with a span of 40 m were chosen, rather than lighter alternatives such as steel beams or steel–concrete composite beams. The application of such structural optimization measures to the arch ribs and structures above the arch collectively resulted in a reduced stress level in the arch ribs. Thus, the stress level in the arch ribs of this SRC arch bridge with a 600 m span was comparable to that of an SRC arch bridge with a span of 400 m (i.e., the Nanpan River Bridge on the Nanning–Kunming High Speed Railway, with a main span of 416 m), as illustrated in Table 9. This reduction in the stress level of the arch ribs yielded a twofold benefit: It diminished the concrete creep and increased the safety margin of the arch.

Since the encasing concrete of the Tian'e Longtan Bridge was poured using a multilayer approach, the compressive stress in

Table 7
Ratio of the dead load to the sum of the dead load and live load of several representative large-span SRC arch bridges.

Bridge classification	Bridge	Main span (m)	Dead load/(dead load + live load)
Highway bridge	Tian'e Longtan Bridge	600	94.6%
	Sichuan Modaoxi Bridge	266	94.2%–95.1%
	Zhaohua Jialing River Bridge	364	94.6%–95.0%
	Xining River Bridge	510	95.8%–96.6%
Railway bridge	Huangtong–Baise Railway Hongshui River Bridge	512	92.0%–93.0%
	Nanning–Kunming High Speed Railway Nanpan River Bridge	416	91.7%

Table 8
Ratio of the weight of the main arch to the weight of the whole superstructure of several representative large-span SRC and CFST arch bridges.

Bridge	Bridge type	Main span (m)	Weight of main arch (t)	Weight of superstructure (t)	Weight of main arch/weight of whole superstructure
Dejiang–Yuqing Highway Wujiang River Bridge	Deck-type CFST arch bridge	475	22 001	38 181	58%
Tian'e Longtan Bridge	Deck-type CFST arch bridge	600	92 000	1 25 000	74%
Yongning Yong River Bridge	Half-through SRC arch bridge	312	13 700	21 600	63%
Daxiaojing Bridge	Deck-type CFST arch bridge	450	22 300	40 700	55%
Nanning–Kunming High Speed Railway Nanpan River Bridge	Deck-type SRC arch bridge	416	69 200	100 700	69%
Shanghai–Kunming High Speed Railway Beipan River Bridge	Deck-type SRC arch bridge	445	69 500	102 500	68%
Bosideng Bridge	Half-through CFST arch bridge	515	21 810	39 000	56%
Hejiang Yangtze River Highway Bridge	Flying-swallow-type CFST arch bridge	507	29 380	38 500	76%
Pingnan Third Bridge	Half-through CFST arch bridge	560	29 620	50 000	59%
Xining River Bridge	Deck-type SRC arch bridge	510	61 230	97 700	63%
Wanzhou Yangtze River Bridge	Deck-type SRC arch bridge	420	26 300	43 500	60%
Zhaohua Jialing River Bridge	Deck-type SRC arch bridge	364	28 400	50 100	57%
Luzhou–Gulin Highway Shuiluo River Bridge	Deck-type reinforced concrete arch bridge	335	32 100	63 200	51%
Leshan–Xichang Highway Suba Bridge	Deck-type SRC arch bridge	350	33 370	60 700	55%

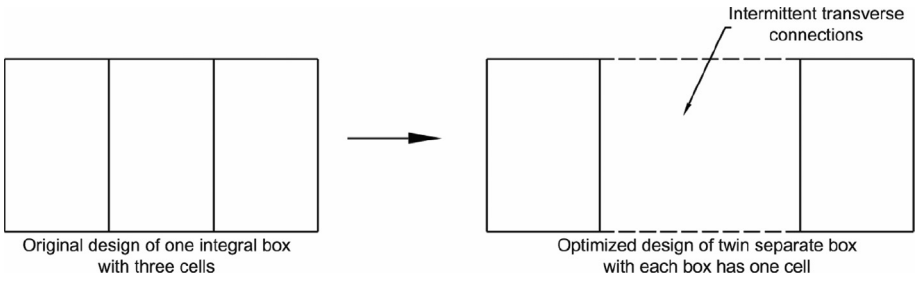

Fig. 20. Optimization of the arch rib section configuration.

the top layer of the encasing concrete was almost zero at the time of the formation of the arch rib. However, there should be some compressive stress reservation in the top layer of concrete to counteract the tensile stress generated by future live loads. To this end, the only choice is to increase the weight of the structures above the arch, especially in the region from the quarter span to the arch crown, which was another reason for adopting prestressed concrete T-type beams instead of light steel beams or steel–concrete composite beams in the Tian'e Longtan Bridge. The minimum compressive stress in the encasing concrete of the Tian'e Longtan Bridge occurs in the top plate at the arch springing section, measuring –3.49 MPa under permanent loads and –0.88 MPa under the standard combination of permanent loads and live loads. The maximum compressive stress of the encasing concrete occurs

Table 9
Comparison of the maximum compressive stresses in the arch ribs of the Tian'e Longtan Bridge versus the Kunming–Nanning High Speed Railway Nanpan River Bridge, with a main span of 416 m.

Location	Dead load (MPa)		Dead load + live load (MPa)	Standard load combination (MPa)
	Nanpan River Bridge	Tian'e Longtan Bridge	Tian'e Longtan Bridge	Tian'e Longtan Bridge
Bottom plates	−18.0	−17.5	−18.5	−20.7
Webs	−16.0	−13.0	−14.0	−15.8
Top plates	−8.7	−9.2	−10.9	−12.6

in the bottom plate at the arch springing section, with values lower than –21 MPa under the standard load combination. These results indicate that the Tian'e Longtan Bridge possesses a significant load-carrying capacity reserve due to its stiffened skeleton and various effective stress-adjustment measures. Furthermore, they suggest the possibility of extending the span length of SRC arch bridges. The above analysis also shows that the traditional concept of using light steel components for spandrel columns and traffic beams may not be suitable for large-span SRC arch bridges, as it not only incurs high cost but also fails to enhance the compressive stress reserve of the top plate in the arch ribs under constant load.

3.6. Longitudinal reinforcement design of the arch ribs

At present, there is a lack of specific design standards for SRC arch bridges. Therefore, the longitudinal reinforcement design of the SRC arch ribs could only rely on the relevant specifications. The concrete strength grade for the arch ribs of the Tian'e Longtan Bridge was C60, according to the Chinese code [21]. Several mainstream design codes for reinforced concrete structures stipulate a minimum longitudinal reinforcement ratio ranging from 0.6% to 1.0% for the entire cross-section of the arch rib [21–25]. However, these regulations do not explicitly clarify whether the specified ratios encompass the steel tube chords of the stiff skeleton or not. Research results have shown that the influence of longitudinal reinforcing bars on the load-bearing capacity and durability of SRC arch ribs is far less than that of steel tubes, and even less than that of stirrups [26]. Consequently, when calculating the longitudinal reinforcement ratio of the arch rib section of an SRC arch bridge, the steel tube chords of the stiff skeleton should be taken into consideration. Given that the steel tube chords alone can easily fulfill the requirements of the minimum longitudinal reinforcement ratio for most SRC arch bridges, only a minimal number of longitudinal reinforcing bars that meet constructional requirements is required for SRC arch ribs.

In addition to specifying the minimum reinforcement ratios, the relevant design specifications propose simplified approximate methods for assessing the ultimate load-bearing capacity of SRC arch sections by considering the material and geometric nonlinearities. To quantify the combined effect of the dual nonlinearities, a simplified moment amplification factor, derived from a differential equation correlating the moment and lateral deformation of the eccentrically compressed rectilinear columns, is employed. Still, even in the case of simple rectilinear columns, notable discrepancies are observed in the moment amplification factors predicted according to different formulas recommended by different specifications. This indicates that the associated theories are still in their infancy. For more complex arch structures, the suitability and validity of the moment amplification factor-based methodology are even more dubious. To be specific, these methods primarily address the moment amplification effect in the vertical deflection while neglecting the impact of horizontal displacement, which generally leads to an overestimation of the moment amplification factor. Moreover, notable disparities emerge in the calculation results according to different standards for reinforced concrete arch structures, as listed in Table 10 [21–25]. The overestimated moment amplification factor would then lead to an improper reinforcement design of the arch ribs. For the Tian'e Longtan Bridge, even when a conservative value of the moment amplification factor of the arch springing section is used, such as 3.61, the calculation results show that the number of longitudinal steel bars required remains very high. In fact, all previous investigations have revealed a moderate moment amplification effect in the concrete arch ribs. For example, a reinforced concrete arch model with a span of 4.5 m, which has been tested by Li [27], indicated that the moment amplification factor was merely 1.039. In addition, independent research conducted by Xie et al. [28] arrived at the conclusion that the arch rib has high stiffness, so secondary moment amplification is unnecessary.

Given the deficiencies in the existing theories, the widely accepted moment amplification factor calculation method proposed by Li [29] was ultimately chosen for the Tian'e Longtan Bridge, and the calculated moment amplification factor of the arch springing section, which controls the design, was 1.51. According to this moment amplification factor, only minimal reinforcing bars that could meet the constructional requirements were required in the longitudinal direction of the arch ribs. The rationality of this design can easily be proved through further scrutiny. First, concrete arch ribs are subjected to small eccentric compression, rendering their sectional mechanical behavior akin to that of prestressed concrete beams. It has been widely accepted that only structural reinforcing bars are required for prestressed concrete beams. Second, the longitudinal reinforcement configuration of the Tian'e Longtan Bridge closely resembles that of two existing large-span SRC arch bridges—namely, the Yongning Yong River Bridge, with a span of 312 m, and the Wanzhou Yangtze River Bridge, with a span of 420 m. These two bridges have been in service for 26 years without displaying any transverse cracks in their arch ribs.

Therefore, it was suggested that, as the SRC arch ribs with a CFST skeleton were subjected to small eccentric compression, the minimum longitudinal reinforcement requirement stipulated by relevant standards could easily be fulfilled due to the presence of the steel tube chords of the stiff skeleton. Thus, the longitudinal

Table 10
Predicted sectional moment amplification factors of the arch ribs of the Tian'e Longtan Bridge using formulas recommended by different design specifications.

Sectional force combination case	Checking section	Design specification				
		JTJ 023-85 [22]	GB 50010-2002 [23]	DIN 1045-3 [24]	BS 5400-4 1990 [25]	JTG 3362-2018 [21]
Maximum moment	Arch springing	2.33	2.23	2.22	2.34	2.12
	L/8	8.39	3.15	3.29	4.85	2.97
	L/4	12.82	5.56	4.82	8.30	4.01
	3*L*/8	7.38	4.19	3.80	6.12	3.66
	Arch crown	3.67	4.43	3.98	6.48	3.87
Maximum axial force	Arch springing	2.24	6.84	5.87	8.59	3.70
	L/8	6.55	4.23	4.22	6.84	3.46
	L/4	7.91	12.62	9.77	19.72	6.76
	3*L*/8	11.77	10.16	8.12	16.53	6.12
	Arch crown	3.50	8.70	7.32	14.65	5.77

JTJ 023-85: code for highway reinforced concrete and prestressed concrete bridges and culverts; GB 50010-2002: code for design of concrete structures; DIN 1045-3: concrete, reinforced and prestressed concrete structures-part 3: execution of structures; BS 5400-4 1990: steel, concrete and composite bridges-part 4: code of practice for design of concrete bridges ; JTG 3362-2018: code for highway reinforced concrete and prestressed concrete bridges and culverts.

reinforcing bars only need to conform to the structural requirements. Meanwhile, it was considered advisable to increase the number of stirrups in the transverse direction and to prestress them when necessary to avoid longitudinal cracking in the encasing concrete.

3.7. Preliminary study on a new SRC arch rib structure

It has been a common practice for the encasing concrete in the arch rib of an SRC bridge to be poured in a multilayer manner, with the web layer concrete being the most difficult to pour. For an arch bridge with a span exceeding 400 m, the casting of the web concrete typically takes two months. Consequently, this results in an approximate two-month disparity in the age of the concrete in adjacent concrete layers. The concrete age difference eventually poses a substantial risk of shrinkage cracking in the subsequent layers of the encasing concrete. If the web concrete layer were to be eliminated, the top concrete layer would be free from the constraints imposed by the web concrete layer. Therefore, similar to the concrete in the bottom layer, the concrete in the top layer would be constrained only by the adjacent concrete segment, with a curing age difference between adjacent segments of only 8–10 days. In addition, removing the web concrete plates could result in a one-third reduction in the quantity of the encasing concrete and thus expedite the construction schedule for the SRC arch ribs by several months. Although the vertical and lateral stiffness of the arch ribs would decrease due to the absence of the web concrete plates, this could be easily compensated for, using other technical measures. Moreover, as the arch ribs are subjected to small eccentric compression with relatively low shear force, it is feasible to replace the concrete web plates with enhanced web members.

Based on the above analysis, a novel composite box arch structure comprising steel tube web members between the top and bottom concrete plates was recently proposed for future SRC arch ribs, as depicted in Fig. 21. This new arch rib structure is derived from the traditional box-shaped SRC arch rib by substituting the concrete web plates with web members made of weather-resistant steel tubes. The web members can be either filled with concrete or left empty. The welding and bolting joints of the stiff skeleton are all embedded between the top and bottom layers of the encasing concrete. The weather-resistant steel web members are as durable as the conventional concrete web plates. Thus, just like the SRC arch, the proposed composite box arch requires no special maintenance. At present, the author's team is actively engaged in conducting a comprehensive analysis, calculations, and experimental validations to substantiate the feasibility of this innovative arch structure.

4. Conclusions

The CFST arch bridge and the SRC arch bridge both fall into the category of concrete arch bridges with a stiff skeleton. The stiff skeleton of the former is a steel tube arch truss, while that of the latter is a CFST arch truss. The Pingnan Third Bridge and the Tian'e Longtan Bridge have been constructed with considerable reserves in terms of the material strength and bearing capacity of the arch ribs. During the construction of these two bridges, the measured arch deflections and steel stresses agreed well with the predicted values from a linear elastic model. Moreover, the most concerning shrinkage cracking of the multilayered cast encasing concrete of the SRC arch ribs has not occurred, as shown in the large-span Wanzhou Yangtze River Bridge and the Yongning Yong River Bridge, which have been in service for over 26 years. Therefore, the extension of the span length of these two types of arch bridges to 700 m based on existing construction methods, materials, and equipment is entirely feasible.

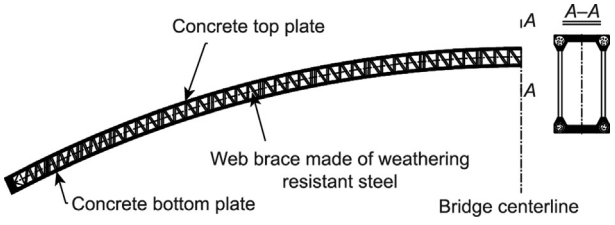

Fig. 21. A new composite box-shape arch structure with weathering resistance steel web braces and concrete top and bottom plates.

A comparative analysis of the technical and economic aspects of two bridges with a similar span length—that is, the Pingnan Third Bridge and the Tian'e Longtan Bridge—revealed the following insights:

(1) The arch rib stiffness of the former is half the stiffness of the latter;

(2) The arch rib weight of the former is one-third the weight of the latter;

(3) The arch rib cost of the former was 70% of the cost of the latter;

(4) The arch ring construction duration of the former was half the duration of the latter;

(5) The total number of days spent on manufacturing the arch ring segments for the former was 70 000 workdays less than the number of days spent for the latter.

This comparison illustrates the main characteristics of these two types of arch bridges. In addition, CFST arch bridges can achieve a remarkable shop production level exceeding 85% and a formwork-free onsite construction. Consequently, the onsite labor requirements can be significantly reduced, and construction convenience is enhanced. In contrast, SRC arch bridges require minimal maintenance throughout their service life, providing longer durability and higher stiffness. Therefore, it is concluded that, if the large-scale stiff skeleton can be manufactured in a shop and transported to the bridge site by water, the CFST arch bridge is the preferable choice among these two types of arch bridges.

Over the past three decades, Chinese engineers have dedicated themselves to the research and construction of CFST arch bridges and SRC arch bridges. Through their sustained efforts, a series of critical technical challenges have been effectively tackled for these two types of arch bridges, significantly reducing the construction risks and boosting the economic competitiveness. As a result, the number and span length of these two types of arch bridges constructed in China have far surpassed those in other countries. These remarkable achievements have not only resulted in significant cost savings but also garnered recognition from the international engineering community.

In the forthcoming research and development of CFST arch bridges, several essential points must be addressed. First, it is imperative to further investigate the feasibility of the novel bolting-welding composite joint for steel tube chords proposed by the author's team. This novel composite joint allows for flange bolt connection outside the tube without affecting the welding connection. It has the potential to reduce high-altitude welding by two-thirds compared with conventional in-tube flange connection, in addition to reducing impediments during the pumping of in-tube concrete. The novel composite joint has been successfully employed in the Tian'e Longtan Bridge and has yet to find application in CFST arch bridges. Second, as illustrated in Section 2.3, significant progress has been achieved in the use of expansion control for the shrinkage compensation of in-tube concrete, which means that the initial compressive stress of the in-tube concrete as a result of expansion can be predesigned. However, questions remain as to the determination of the appropriate magnitude of

the compressive stress reserve of the in-tube concrete. Striking the right balance in this regard is crucial, as excessive compressive stress could be detrimental to the straight welded seams of the steel tubes, while insufficient compressive stress reserve might lead to delamination between the steel tubes and the in-tube concrete during future intense temperature fluctuations.

With respect to SRC arch bridges, further research efforts should be directed toward methods aimed at reducing the volume of the encasing concrete supported by the stiff skeleton. There is also a need to enhance the mechanization level of several critical construction phases, including formwork and steel bar installation and concrete pouring, with the ultimate goal of minimizing labor requirements. In conclusion, arch bridge construction technologies should be further innovated by continuously identifying and addressing challenges and finding solutions encountered during engineering practice.

Acknowledgments

The author would like to thank Chief Engineer and Professor-level Senior Engineer Dayan Qin, Professor-level Senior Engineer Hailong Du and Senior Engineer Xiaobin Luo of Guangxi Road and Bridge Engineering Group Co., Ltd., Deputy Chief Engineer and Professor-level Senior Engineer Congjin Shang of Guangxi Communications Design Group Co., Ltd. (China), Chief Engineer and Professor-level Senior Engineer Tingmin Mu of Sichuan Communication Planning, Survey, Design and Research Institute Ltd. (China), and Professor-level Senior Engineer Longlin Wang of Guangxi Transportation Science and Technology Group Co., Ltd. (China) for providing materials and pictures for this paper, and thank for Professor Zheng Chen and Senior Engineer Xiao Guo of Guangxi University (China) for writing assistance. The paper was translated and proofread by Associate Professor Bing Tu of Guangxi University and Associate Professor Min Wang of Chongqing Jiaotong University (China), and was financially supported by the Guangxi Key Research and Development Plan Program (AB22036007).

References

[1] Zheng JL, Wang JJ. Concrete-filled steel tube arch bridges in China. Engineering 2018;4(1):143–55.
[2] Zheng JL, Wang JJ, Mou TM, Feng Z, Han Y, Qin DY. Feasibility study on design and construction of concrete filled steel tubular arch bridge with a span of 700 m. Strategic Study CAE 2014;16(8):33–7. Chinese.
[3] Zheng JL. Discussion on technology of suspending and connecting for the RC bridge with an unusual big span. China J Highw Transp 1999;12(1):42–9. Chinese.
[4] Chen BC, Yang YL. Investigation and analysis of concrete-filled steel tube arch bridges. World Bridges 2006;2:73–7. Chinese.
[5] Zheng JL, Han Y, Qin DY, Feng Z, Luo YF, Pang BX, et al., inventors; Guangxi Road and Bridge Engineering Group Co., Ltd, assignee. Vacuum-assisted perfusion method and infusion system of concrete in large concrete-filled steel tube. China patent CN 201210184040. 2013 May 15.
[6] Zheng JL, Wang JJ, Feng Z, Han Y, Qin DY. Vacuum aided concrete grouting process test of concrete filled steel tube arch segment. China J Highw Transp 2014;27(6):44–50.
[7] Liu JP, Zhou DL, Ran QP, Yang Y, Liu JZ, inventors; Jiangsu Sobute New Materials Co. Ltd., Bute Building Materials (Tianjin) Co., Ltd, assignees. A slump-guaranteed polycarboxylic acid-type superplasticizer. China patent CN 102976655B. 2012 Aug 29.
[8] Cheng Z, Cheng B, Wu CJ, Li KL, Li J, Nong YM, et al., inventors; Guangxi University, assignee. Concrete mix design method based on regulation of pouring construction performance. China patent CN 113910447B. 2012 Oct 21.
[9] Liu JP, Wang YJ, Tian Q, Zhang SZ. Temperature sensitivity of light calcined magnesia expansion agent and its mechanism analysis. J Southwest Univ 2011;41(2):359–64. Chinese.
[10] Liu JP, Xu W, Wang YJ, Yao T, Li M, Tian Q, inventors; Jiangsu Sobute New Materials Co. Ltd., assignee. A specific admixture for self-compacting and non-shrink concrete in concrete-filled steel tubular structures. China patent CN 107200500B. 2019 Dec 27.
[11] Zheng JL, Zhang Z, Mei GX, Huang DG, Mi DC, inventors; Guangxi University, assignee. Construction method suitable for long-span arch bridge foundation. Nederland patent NLB 12031612. 2023 Apr 3.
[12] Wang TC, Yang JH, Zhang Z, Duan YR, Mei GX. Seismic behavior of arch bridge abutments under sandy–gravel foundations with different grouting depths: insights from shaking table tests. J Bridge Eng 2023;28(7):05023003.
[13] Zheng JL, Deng NC, Wang JJ, Yang ZF, Han Y, Li CX, et al., inventors; Guangxi Road and Bridge Engineering Group Co., Ltd, Guangxi University, assignee. A displacement control system and its application method of cable crane tower for arch bridge construction. China patent CN 107620260B. 2018 Jun 1.
[14] Qin DY, Zheng JL, Du HL, Han Y, Kui LJ. Optimization method and application of for one time tensioning of buckle cables in cable-stayed buckle system. China Railw Sci 2020;41(6):52–60. Chinese.
[15] Qin DY, Du HL, Han Y, Luo XB, Zheng J, Wu GG, et al., inventors; Guangxi Road and Bridge Engineering Group Co., Ltd, assignee. An optimized calculation method for cantilever assembly construction of arch bridges. China patent CN 108038326B. 2020 Jul 24.
[16] Qin DY, Zheng JL, Du HL, Han Y, Luo XB, Wu GG, et al., inventors; Guangxi Road and Bridge Engineering Group Co., Ltd, assignee. An efficient method for loosening buckle cables of arch ribs. China patent CN 111321666B. 2020 Oct 30.
[17] Ministry of Housing and Urban-Rural Development, General Administration of Quality Supervision, Inspection and Quarantine of the People's Republic of China. GB 50923-2013: Technical code for concrete-filled steel tube arch bridges. Chinese standard. Beijing: China Planning Press; 2014. Chinese.
[18] Ministry of Transport of the People's Republic of China. JTG/T D65–06-2015: Specifications for design of highway reinforced concrete-filled steel tubular arch bridges. Chinese standard. Beijing: China Communication Press; 2015. Chinese.
[19] National Railway Administration of the People's Republic of China. TB 10091-2017: Code for design on steel structure of railway bridge. Chinese standard. Beijing: China Railway Press; 2017. Chinese.
[20] Japanese Civil Engineering Society. Construction of the Teishicho Bridge—a 600 meter-span long arch bridge. Japanese standard. Tokyo: the Association; 2003. Japanese.
[21] Ministry of Transport of the People's Republic of China. JTG 3362-2018: Code for highway reinforced concrete and prestressed concrete bridges and culverts. Chinese standard. Beijing: China Communication Press; 2018. Chinese.
[22] Ministry of Transport of the People's Republic of China. JTJ 023-85: Code for highway reinforced concrete and prestressed concrete bridges and culverts. Chinese standard. Beijing: China Communication Press; 1985. Chinese.
[23] Ministry of Housing and Urban-Rural Development, General Administration of Quality Supervision, Inspection, Quarantine of the People's Republic of China. GB 50010-2002: Code for design of concrete structures. Chinese standard. Beijing: China Architecture & Building Press; 2002. Chinese.
[24] DE-DIN. DIN 1045-3: Concrete, reinforced and prestressed concrete structures-part 3: execution of structures. German standard. Berlin: Beuth Verlag Berlin; 2005. German.
[25] Civil Engineering and Building Structures Standards Committee. BS5400-4 1990: Steel, concrete and composite bridges—part 4: code of practice for design of concrete bridges. British standard. London: British Standard Institute; 1990.
[26] Yao GH, Li YJ, Liao FY. Behavior of concrete-filled steel tube reinforced concrete columns subjected to axial compression. J Build Struct 2013;34(5):114–21. Chinese.
[27] Li J. The study on moment magnification factor of reinforced concrete arch bridge [dissertation]. Chengdu: Southwest Jiaotong University; 2012.
[28] Xie YF, Che HM, He GH, Lu HL. Railway reinforced concrete bridge. Beijing: China Railway Press; 1982. Chinese.
[29] Li GH. Stability and vibration of bridge structures. Beijing: China Railway Press; 1992. Chinese.